The
Iowa State College
Bulletin

Bulletin No. 182

STRUCTURAL BEHAVIOR OF A PLATE RESEMBLING A CONSTANT THICKNESS BRIDGE ABUTMENT WINGWALL

by H. P. Harrenstien
W. C. Alsmeyer

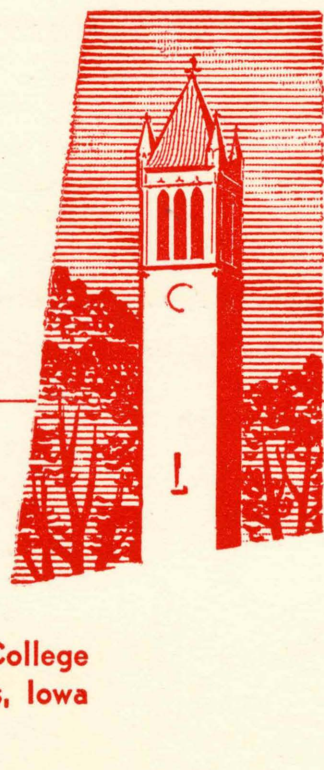

IOWA ENGINEERING EXPERIMENT STATION

Iowa State College
Ames, Iowa

THE IOWA ENGINEERING EXPERIMENT STATION

The Iowa Engineering Experiment station was organized in 1904 for the purpose of conducting investigations that would aid in the industrial development of the area, and for carrying on an experimental program on engineering problems encountered in public administration.

The Station is engaged in the investigation of fundamental engineering problems, and in the development of industrial processes to utilize further the raw materials of the area or to develop products of use to the people of the state and nation. This work is carried on in the fields of agriculture, chemical, ical engineering and theo

The d to industries within ar s stated above. For furtl

T TION

STRUCTURAL BEHAVIOR OF A PLATE RESEMBLING A CONSTANT THICKNESS BRIDGE ABUTMENT WINGWALL

by

H. P. Harrenstien, Instructor of Civil Engineering

and

W. C. Alsmeyer, Formerly Associate Professor of Civil Engineering

Bulletin 182

of the

Iowa Engineering Experiment Station

Price: Seventy-five cents

THE IOWA STATE COLLEGE BULLETIN

Ames, Iowa

Vol. LVII	January 14, 1959	No. 33

Published weekly by Iowa State College of Agriculture and Mechanic Arts, Ames, Iowa. Entered as second-class matter and accepted for mailing at the special rate of postage provided for in Section 429, P. L. & R., Act of August 24, 1912, authorized April 12, 1920.

INTRODUCTION

Many highway and railway bridges are supported on reinforced concrete abutments similar to the one shown in figure 1. This type of abutment is used by the Iowa State Highway Commission. The wingwalls of this abutment, which may be either of constant or variable thickness, are the vertical slabs of reinforced concrete attached to the breastwall and footings. A distributed load of varying intensity is exerted on these slabs by the lateral pressure of the soil which they retain. In addition to being retaining walls, the wingwalls also function as counterforts to the breastwall of the abutment. As might be expected, the structural action of such a wall is very complex; for that reason it does not lend itself readily to common methods of structural engineering analysis.

The practice of the Iowa State Highway Commission is to assume that the wingwall is a thin homogeneous plate which is subjected to a normal distributed load which varies linearly with depth. The commission considers the plate as fixed at the juncture to the breastwall and footing and free on the other two edges. Since such a plate has mathematical boundary conditions which are quite complex, a solution of the governing differential plate equation is not easily obtained. Most structural engineers do not have the time necessary to solve such a plate problem. Therefore bridge engineers make various additional simplifying assumptions as to the structural behavior of these wingwalls to obtain practical designs. The assumptions and the resulting designs vary greatly with individual engineers.

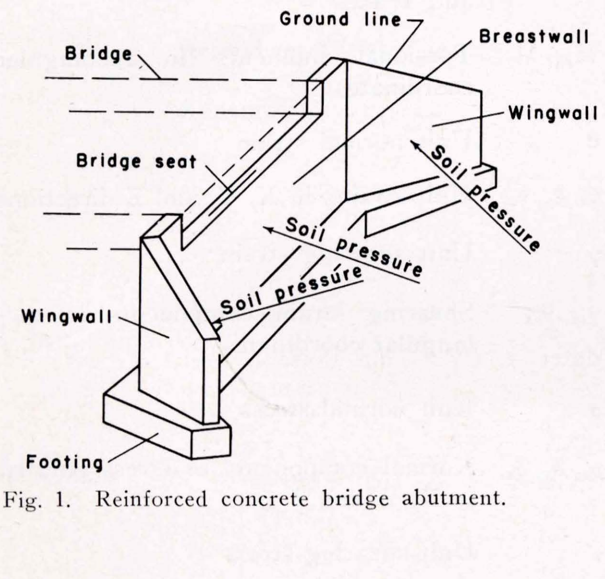

Fig. 1. Reinforced concrete bridge abutment.

The first stage of this project was a literature review and a questionaire survey. A thorough and exhaustive search was made in all publications for material on the subject of bridge abutments and wingwalls. All of the several hundred available publications were reviewed; but no experimental or rigorous analytical investigations of reinforced concrete wingwalls of the type shown in figure 1 were found. The findings agreed with those of the Portland Cement Association (11, p.12) that "no structural analysis is available by which the stresses (in wingwalls) may be determined", and "suitable reinforcement may be provided by judgment or empirical rules". Letters and questionnaires similar to the ones shown in the Appendix were sent to several hundred highway, railway, and consulting engineers throughout the United States and Canada. Answers were returned by 80% of the highway engineers, 59% of the railway bridge engineers and 67% of the consulting engineers. These answers are tabulated in the Appendix.

The results of both the literature review and the survey confirm the fact that individual engineers analyze and design such wingwalls on the basis of different assumptions regarding the structural behavior of these walls. The major result of the first stage of the project was the compilation of evidence that a thorough study of this subject was needed.

The second stage of this project establishes a feasible analytical method for the solution of the type of plate problem associated with a wingwall. An aluminum plate of constant thickness, considered as a model of a typical wingwall, was studied both analytically and experimentally. An exact solution of the basic plate equation was not considered feasible because of the complex boundary conditions involved, but a numerical solution using the method of finite differences was obtained. An experimental study was made of the aluminum plate to serve as a control in determining the refinement of the numerical solution necessary to produce adequate theoretical results for a particular shape of plate.

THEORETICAL INVESTIGATION

Lagrange's differential equation governs the small deflections of a flat constant thickness thin plate which is subjected to normal distributed loads. This equation whose development may be found in various sources, [13, 15, 17], may be written as follows:

$$\frac{\partial^4 w}{\partial x^4} + 2\frac{\partial^4 w}{\partial x^2 \partial y^2} + \frac{\partial^4 w}{\partial y^4} = \frac{p}{D}$$

where x, y = coordinates of a point
p = intensity of distributed load at x, y
w = deflection of plate at any point x, y
$D = \dfrac{Eh^3}{12(1-\mu^2)}$
and E = modulus of elasticity
h = thickness of plate
μ = Poisson's ratio

The limitations and assumptions on this equation are as follows:

a. The plate is medium-thick, i.e., not so thin that it approaches a membrane in action nor so thick that the distribution of stresses at the ends appreciably influences the results.

b. The material is homogeneous, isotropic, and perfectly elastic.

c. A straight line perpendicular to the central surface of the plate before flexure remains straight and perpendicular to that surface after flexure.

d. Stress is proportional to strain.

A solution of this equation would permit rather precise predictions of structural behavior of plates with due regard to the previous assumptions; hence this equation forms the basis for all attempts at exact solutions of plate problems. Unfortunately, it has been solved only for a few particular cases, most of which involve symmetry or simplified loading and boundary conditions. An exact mathematical solution of this differential equation for a plate of the wingwall type is difficult, if not impossible.

It was felt that for the case of a reinforced concrete wingwall, certain approximate solutions to the above equation would yield results which were as valid as those of the so-called exact solution. Some of the various approximate methods considered were the "Elastic Web", the "Trial-Load", "Moment Distribution", the Presan Photographic Model Analysis, and the Finite-Difference method.

The Elastic-Web method [7,19] conceives the plate as a network of orthogonally crossed elastic wires. The loads, if of the distributed type, are replaced by equivalent concentrations at the web intersections. End conditions representing different conditions of continuity or freedom from restraint at the supports are determined from the theory of the action of elastic webs, which follows the theory of thin membranes. The deflections of the web under various loading conditions give moments, stresses, and deflections of the plate much as the equilibrium polygon can be made to yield analagous quantities for beams. The deflections of the web are determined by means of difference equations that are easily set up. The number of the difference equations that must be solved simultaneously is usually equal to the number of web intersections.

In the Trial Load method of analysis [16, 18] the plate is reduced to a number of isolated beams running at right angles to each other. The load on the plate is so distributed to these crossed beams that final deflections and positions of the beams are compatible. Either a trial and error method of procedure may be used to obtain these compatible deflections or simultaneous equations may be written from which results may be obtained.

The Moment Distribution method [4, 2] superimposes a grid on the plate and uses a process similar to that of the familiar moment distribution in planar structures. Separate distribution must be made of the fixed end moments resulting from unit displacements for each joint. Then reactions or holding forces for each of these solutions must be calculated at these joints; and, finally, to obtain the deflections, a set of simultaneous equations which satisfy shear relationships must be solved. The number of these equations is equal to the number of node points corresponding to grid intersections.

The Presan method [3] consists of building a lucite model of the plate to be analyzed and then coating one surface with reflective paint. A gridwork is constructed and placed parallel to this reflective surface some distance away. The grid is reflected by the model to a camera. When pressure is applied to the lucite plate, the reflection of the grid to the camera is distorted. Photographs of the reflected grid are taken before and after loading. From these photographs slopes of the lucite plate may be determined. Using these slopes and finite difference equations the plate may be analyzed.

The finite difference method [17, pp. 106-143] is a very powerful numerical method for the approximate solution of differential equations. Its application to the Lagrange equation consists of rewriting the differential equation in terms of unknown values of the deflection at a finite number of points on the plate, usually corresponding to the intersections of superimposed grid lines. The use of this method results directly in the formulation of one simultaneous linear algebraic equation for each grid intersection or node point.

The decision was made to use this finite difference method; since simultaneous equations may be formulated directly instead of after long laborious, analogous manipulations. The high-speed digital computer has made the solution of these simultaneous equations practical, convenient, and in most cases economical.

The Lagrange plate equation as mentioned previously is:

$$\frac{\partial^4 w}{\partial x^4} + 2\frac{\partial^4 w}{\partial x^2 \partial y^2} + \frac{\partial^4 w}{\partial y^4} = \frac{P}{D}$$

Expressions for moments, etc. are:

$$\text{Moments:}\quad M_x = -D\left(\frac{\partial^2 w}{\partial x^2} + \mu\frac{\partial^2 w}{\partial y^2}\right)$$

$$M_y = -D\left(\frac{\partial^2 w}{\partial y^2} + \mu\frac{\partial^2 w}{\partial x^2}\right)$$

$$M_{xy} = M_{yx} = D(1-\mu)\frac{\partial^2 w}{\partial x \partial y}$$

$$\text{Shears:}\quad Q_x = -D\left(\frac{\partial^3 w}{\partial y^3} + \frac{\partial^3 w}{\partial x \partial y^2}\right)$$

$$Q_y = -D\left(\frac{\partial^3 w}{\partial x^3} + \frac{\partial^3 w}{\partial y \partial x^2}\right)$$

$$\text{Edge Force:}\quad R_x = -D\left[\frac{\partial^3 w}{\partial x^3} + (2-\mu)\frac{\partial^3 w}{\partial x \partial y^2}\right]$$

$$R_y = -D\left[\frac{\partial^3 w}{\partial y^3} + (2-\mu)\frac{\partial^3 w}{\partial y \partial x^2}\right]$$

$$\text{Concentrated Corner Force:}\quad R = 2M_{xy} = 2D(1-\mu)\frac{\partial^3 w}{\partial x \partial y}$$

where moments and shears are for a unit length of edge and where notation and limitations are as previously stated.

The directions corresponding to positive quantities are shown in the following sketch:

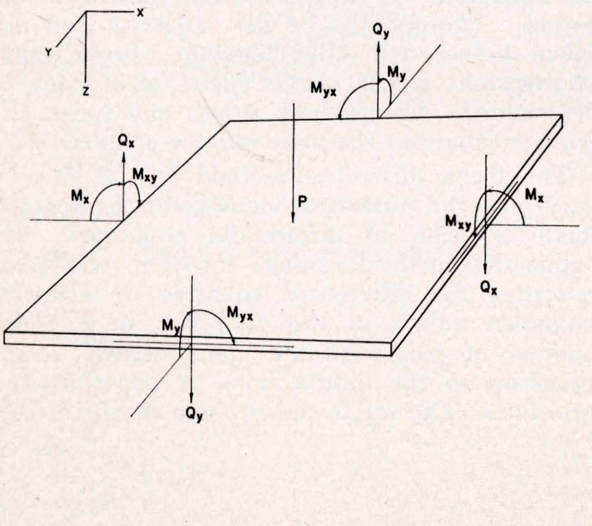

Consider the following network which may be drawn on the surface of the deflected plate.

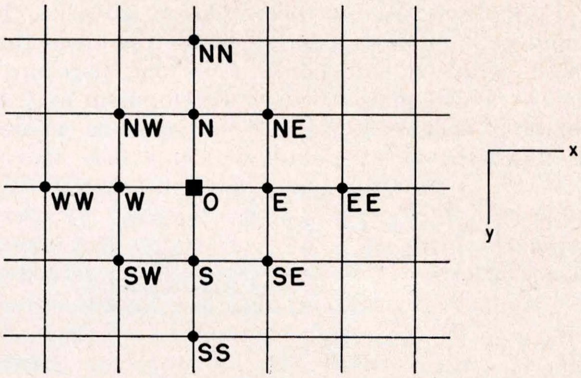

Fig. 2. Grid network.

The elevation of the section line through point o in the E-W direction may be drawn as follows:

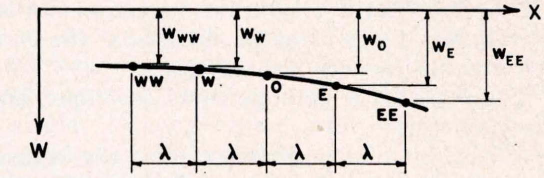

The slope at point o may be approximated in several ways. In general, any of the following forms may be used:

$$\left[\frac{\partial w}{\partial x}\right]_o \doteq \frac{w_E - w_O}{\lambda}\quad \text{, the first forward difference quotient;}$$

$$\left[\frac{\partial w}{\partial x}\right]_o \doteq \frac{w_O - w_W}{\lambda}\quad \text{, the first backward difference quotient;}$$

$$\left[\frac{\partial w}{\partial x}\right]_o \doteq \frac{w_E - w_W}{2\lambda}\quad \text{, the first central difference quotient.}$$

For particular situations, one form may be more accurate than the others. In general, however, without any other information, there is no particular preference. The first central difference quotient will be used here.

To approximate the second derivative in the x-direction at o, again there is a choice of forms. As an obvious extension of the first central difference quotient, the second derivative may be approximated by taking the first central difference quotient of the first central difference quotient. Thus

$$\left[\frac{\partial^2 w}{\partial x^2}\right]_o \doteq \frac{1}{4\lambda^2}\left[(w_{EE} - w_O) - (w_O - w_{WW})\right]$$

However, this form involves values of w at points which are two grid points removed from the point of interest, o. The second derivative at o will obviously depend more on the values of w at E and W than at points farther removed. This factor may be taken into account by approximating the second derivative by taking the first forward difference quotient of the first backward difference quotient, or vice versa since both operations give the same form for equal grid spacings. Thus:

$$\left[\frac{\partial^2 w}{\partial x^2}\right]_o \doteq \frac{1}{\lambda}\left(\frac{w_E - w_o}{\lambda} - \frac{w_o - w_W}{\lambda}\right) = \frac{1}{\lambda^2}\left(w_E - 2w_o + w_W\right)$$

Consistent with the above, the third derivative may be approximated by

$$\left[\frac{\partial^3 w}{\partial x^3}\right]_o \doteq \frac{1}{2\lambda}\left[\frac{1}{\lambda^2}\left(w_{EE} - 2w_E + w_o\right) - \frac{1}{\lambda^2}\left(w_o - 2w_W + w_{WW}\right)\right]$$

$$\doteq \frac{1}{2\lambda^3}\left(w_{EE} - 2w_E + 2w_W - w_{WW}\right)$$

and the fourth derivative by

$$\left[\frac{\partial^4 w}{\partial x^4}\right]_o \doteq \frac{1}{\lambda^2}\left\{\left[\frac{\partial^2 w}{\partial x^2}\right]_E - 2\left[\frac{\partial^2 w}{\partial x^2}\right]_o + \left[\frac{\partial^2 w}{\partial x^2}\right]_W\right\}$$

$$\doteq \frac{1}{\lambda^4}\left[\left(w_{EE} - 2w_E + w_o\right) - 2\left(w_E - 2w_o + w_W\right) + \left(w_o - 2w_W + w_{WW}\right)\right]$$

$$\doteq \frac{1}{\lambda^4}\left(w_{EE} - 4w_E + 6w_o - 4w_W + w_{WW}\right)$$

The mixed second derivative may be approximated by

$$\left[\frac{\partial^2 w}{\partial x\, \partial y}\right]_o \doteq \frac{1}{2\lambda}\left[\left(\frac{w_{SE} - w_{SW}}{\lambda^2}\right) - \left(\frac{w_{NE} - w_{NW}}{\lambda^2}\right)\right]$$

$$\doteq \frac{1}{2\lambda^3}\left(w_{SE} - w_{NE} - w_{SW} + w_{NW}\right)$$

The mixed fourth derivative becomes

$$\left[\frac{\partial^4 w}{\partial x^2 \partial y^2}\right]_o \doteq \frac{1}{2}\left\{\left[\frac{\partial^2 w}{\partial x^2}\right]_S - 2\left[\frac{\partial^2 w}{\partial x^2}\right]_o + \left[\frac{\partial^2 w}{\partial x^2}\right]_N\right\}$$

$$\doteq \frac{1}{\lambda^2}\left[\left(\frac{w_{SE} - 2w_S + w_{SW}}{\lambda^2}\right) - 2\left(\frac{w_E - 2w_o + w_W}{\lambda^2}\right) + \left(\frac{w_{NE} - 2w_N + w_{NW}}{\lambda^2}\right)\right]$$

$$\doteq \frac{1}{\lambda^4}\left[w_{NE} + w_{SE} + w_{SW} + w_{NW} - 2\left(w_N + w_S + w_E + w_W\right) + 4w_o\right]$$

Hence the approximate values of the partial derivatives at point o may be written in terms of the deflection at o and neighboring points with reference to figure 2 as follows:

$$\left[\frac{\partial w}{\partial x}\right]_o = \frac{1}{2\lambda}\left(w_E - w_W\right)$$

$$\left[\frac{\partial^2 w}{\partial x^2}\right]_o = \frac{1}{\lambda^2}\left(w_E - 2w_o + w_W\right)$$

$$\left[\frac{\partial^3 w}{\partial x^3}\right]_o = \frac{1}{2\lambda^3}\left(w_{EE} - 2w_E + 2w_W - w_{WW}\right)$$

$$\left[\frac{\partial^4 w}{\partial x^4}\right]_o = \frac{1}{\lambda^4}\left(w_{EE} - 4w_E + 6w_o - 4w_W + w_{WW}\right)$$

$$\left[\frac{\partial w}{\partial y}\right]_o = \frac{1}{2\lambda}\left(w_S - w_N\right)$$

$$\left[\frac{\partial^2 w}{\partial y^2}\right]_o = \frac{1}{\lambda^2}\left(w_S - 2w_o + w_N\right)$$

$$\left[\frac{\partial^3 w}{\partial y^3}\right]_o = \frac{1}{2\lambda^2}\left(w_{SS} - 2w_S + 2w_N - w_{NN}\right)$$

$$\left[\frac{\partial^4 w}{\partial y^4}\right]_o = \frac{1}{\lambda^4}\left(w_{SS} - 4w_S + 6w_o - 4w_N + w_{NN}\right)$$

$$\left[\frac{\partial^2 w}{\partial x \partial y}\right]_o = \frac{1}{4\lambda^2}\left(w_{SE} - w_{NE} - w_{SW} + w_{NW}\right)$$

$$\left[\frac{\partial^4 w}{\partial x^2 \partial y^2}\right]_o = \frac{1}{\lambda^4}\Big[w_{NE} + w_{SE} + w_{SW} + w_{NW} - 2\left(w_N + w_S + w_E + w_W\right) + 4w_o\Big]$$

Where $\lambda =$ Spacing of square network (in.).

If these approximate values of derivatives are substituted into the appropriate differential equations from the plate theory, the following expressions result:

Load: $$20\, w_o - 8\left(w_N + w_E + w_S + w_W\right) + 2\left(w_{NE} + w_{SE} + w_{SW} + w_{NW}\right) + w_{NN} + w_{EE} + w_{SS} + w_{WW} = \frac{p_o \lambda^4}{D}$$

Moments: $$\left(M_x\right)_o = -\frac{D}{\lambda^2}\Big[-(2 + 2\mu)\, w_o + w_W + w_E + \mu\left(w_N + w_S\right)\Big]$$

$$\left(M_y\right)_o = -\frac{D}{\lambda^2}\Big[-(2 + 2\mu)\, w_o + w_N + w_S + \mu\left(w_W + w_E\right)\Big]$$

$$\left(M_{xy}\right)_o = \frac{D(1-\mu)}{4\lambda^2}\left(w_{SE} - w_{NE} - w_{SW} + w_{NW}\right)$$

Shears: $$\left(Q_x\right)_o = -\frac{D}{2\lambda^3}\Big[4\left(w_W - w_E\right) + w_{NE} + w_{SE} - w_{NW} - w_{SW} - w_{WW} + w_{EE}\Big]$$

$$\left(Q_y\right)_o = -\frac{D}{2\lambda^3}\Big[4\left(w_N - w_S\right) + w_{SE} + w_{SW} - w_{NW} - w_{NE} - w_{NN} + w_{SS}\Big]$$

Edge Forces: $$\left(R_x\right)_o = -\frac{D}{2\lambda^3}\Big[(6 - 2\mu)\left(w_W - w_E\right) + (2-\mu)\left(w_{NE} + w_{SE} - w_{NW} - w_{SW}\right) - w_{WW} + w_{EE}\Big]$$

$$\left(R_y\right)_o = -\frac{D}{2\lambda^3}\Big[(6 - 2\mu)\left(w_N - w_S\right) + (2-\mu)\left(w_{SE} + w_{SW} - w_{NW} - w_{NE}\right) - w_{NN} + w_{SS}\Big]$$

Corner Force: $$\left(R\right)_o = \frac{D(1-\mu)}{2\lambda^2}\left(w_{SE} - w_{NE} - w_{SW} + w_{NW}\right)$$

The boundary conditions to be considered here correspond to those for fixed and free edges. Conditions which are assumed on these boundaries are specified on the following page.

1. Fixed Edge on which y = zero:

$$\left.\begin{aligned}&\text{Deflection Zero: } w = 0\\ &\text{Slope Zero } \quad \frac{\partial w}{\partial x} = 0\end{aligned}\right\} \text{ at } x = 0$$

2. Free Edge on which y = constant:

Moment Zero: $M_y = 0 = \dfrac{\partial^2 w}{\partial y^2} + \mu \dfrac{\partial^2 w}{\partial x^2}$

Edge Forces: R_y

$$= -D\left[\frac{\partial^3 w}{\partial y^3} + (2-\mu)\frac{\partial^3 w}{\partial y \partial x^2}\right]$$

3. Free Corner:

Moment Zero: $M_x = M_y = 0;\ \dfrac{\partial^2 w}{\partial x^2}$

$$= \frac{\partial^2 w}{\partial y^2} = 0$$

Edge Force: R_x

$$= -D\left[\frac{\partial^3 w}{\partial x^3} + (2-\mu)\frac{\partial^3 w}{\partial y^2 \partial x}\right]$$

$$R_y = -D\left[\frac{\partial^3 w}{\partial y^3} + (2-\mu)\frac{\partial^3 w}{\partial y \partial x^2}\right]$$

Corner Force: $R = 2D(1-\mu)\dfrac{\partial^2 w}{\partial x \partial y}$

In terms of finite differences, these boundary conditions may be expressed as,

1. Fixed Edge on which y = zero:

$$w_o = 0$$

$$w_E - w_W = 0$$

2. Free Edge on which y = constant:

$$-(2 + 2\mu)w_o + w_N + w_S + \mu(w_W + w_E) = 0$$

$$(6 - 2\mu)(w_N - w_S) + (2-\mu)(w_{SE} + w_{SW} - w_{NW} - w_{NE}) - w_{NN} + w_{SS} = -\frac{2\lambda^3 (R_y)_o}{D}$$

3. Free Corner:

$$w_E - 2w_o + w_W = 0$$

$$w_S - 2w_o + w_N = 0$$

$$(6 - 2\mu)(w_W - w_E) + (2-\mu)(w_{NE} + w_{SE} - w_{NW} - w_{SW}) - w_{WW} + w_{EE} = -\frac{2\lambda^3 (R_x)_o}{D}$$

$$(6 - 2\mu)(w_N - w_S) + (2-\mu)(w_{SE} + w_{SW} - w_{NW} - w_{NE}) - w_{NN} + w_{SS} = -\frac{2\lambda^3 (R_y)_o}{D}$$

$$w_{SE} - w_{NE} - w_{SW} + w_{NW} = \frac{2\lambda^2 (R)_o}{D(1-\mu)}$$

Since w_o in each boundary condition is for a point on the edge of the plate, it is apparent that some of the deflections indicated are fictitious ones lying off the plate. To indicate the procedure used to express these fictitious deflections in terms of real ones let us consider the example of a point on the edge where y = constant. One may see from the diagrams below that there are deflections at four points off the plate in the equation for the edge force.

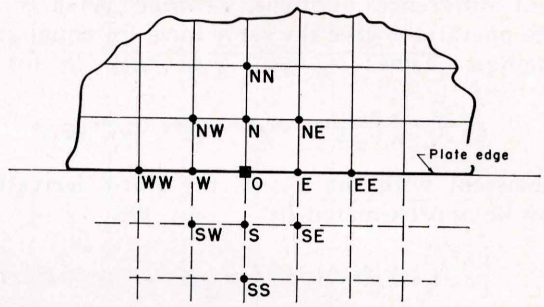

The fictitious deflections are w_{sw}, w_s, w_{se}, and w_{ss}.

These fictitious deflections may be evaluated in terms of the deflections of the plate so that the conditions for a free edge can be determined in terms of deflections at points on the plate. Since four quantities are to be eliminated, five conditions are specified along the free edge. They are:

1. Load: $20w_o - 8(w_N + w_E + w_S + w_W) + 2(w_{NW} + w_{NE} + w_{SE} + w_{SW}) + w_{WW} + w_{NN} + w_{EE} + w_{SS} = \dfrac{p_o \lambda^4}{D}$

2. Edge Force: $(6 - 2\mu)(w_N - w_S) + (2-\mu)(w_{SE} + w_{SW} - w_{NW} - w_{NE}) - w_{NN} + w_{SS} = -\dfrac{2\lambda^3 (R_y)_o}{D}$

3. Moment at o: $-(2 + 2\mu)w_o + w_N + w_S + \mu(w_W + w_E) = 0$

Moment at w: $-(2 + 2\mu)w_W + w_{NW} + w_{SW} + \mu(w_{WW} + w_o) = 0$

Moment at E: $-(2 + 2\mu)w_E + w_{NE} + w_{SE} + \mu(w_{EE} + w_o) = 0$

(For an edge with no loading $p_o = (R_y)_o = 0$)

Eliminating w_{ss}, w_{sw}, w_{se}, and w_s from these equations gives:

$$(16 - 8\mu - 6\mu^2)w_o + (-12 + 4\mu)w_N + (-8 + 4\mu + 4\mu^2)(w_W + w_E) + (4 - 2\mu)(w_{NE} + w_{NW}) + (1 - \mu^2)(w_{WW} + w_{EE}) + 2w_{NN} = \frac{p_o \lambda^4}{D} + \frac{2\lambda^3 (R_y)_o}{D}$$

The equation for this edge condition may be schematically represented as follows:

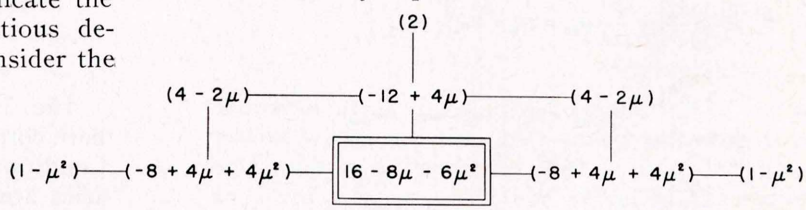

This procedure was followed for all typical points of a plate resembling a wingwall (with simplified upper edge) and the various quantities were evaluated for $\mu = 0.30$. Resulting coefficient patterns for these typical points are included in figure 3. Among these patterns are included for reference purposes points for edge conditions which are not specifically used in this investigation.

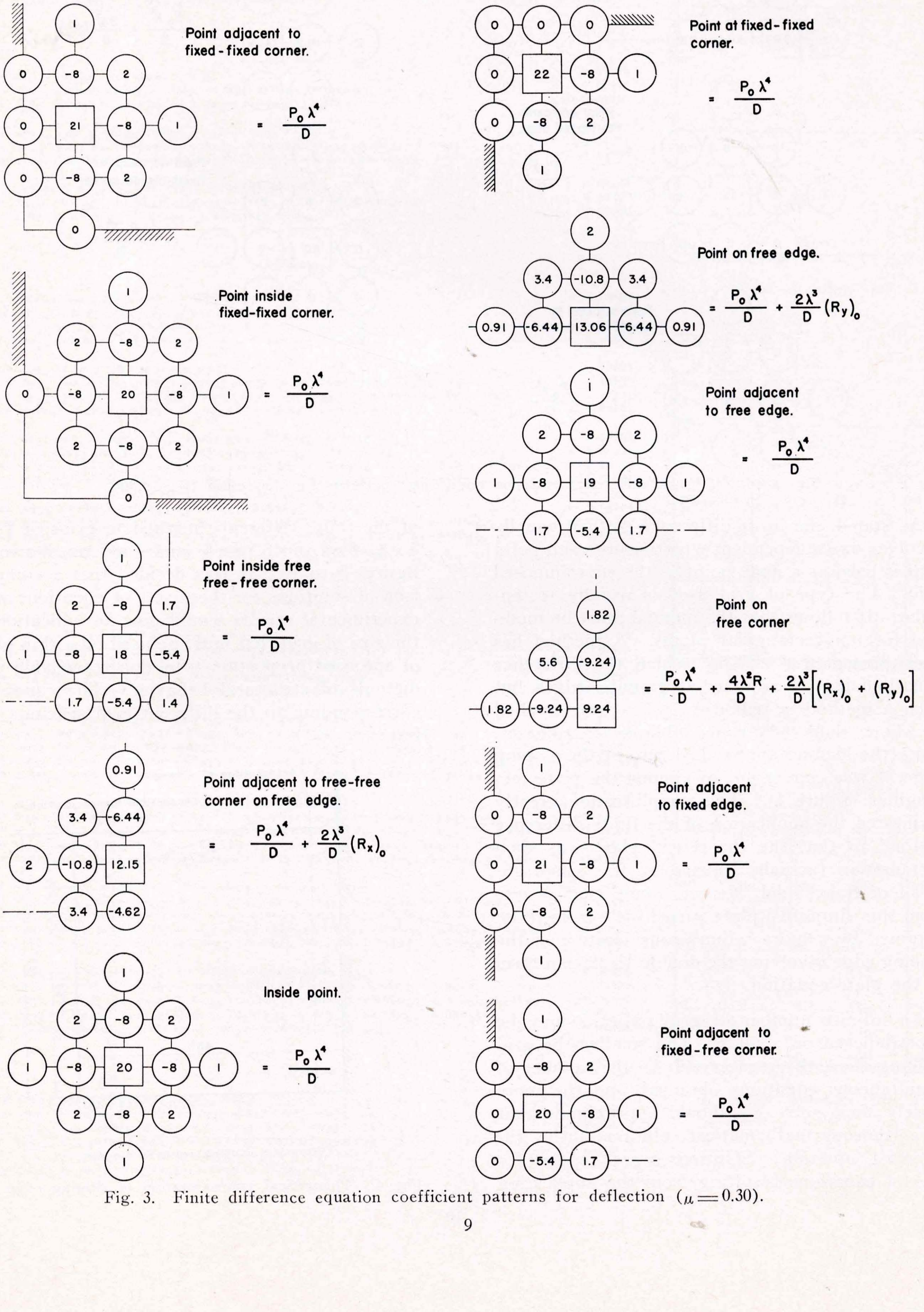

Fig. 3. Finite difference equation coefficient patterns for deflection ($\mu = 0.30$).

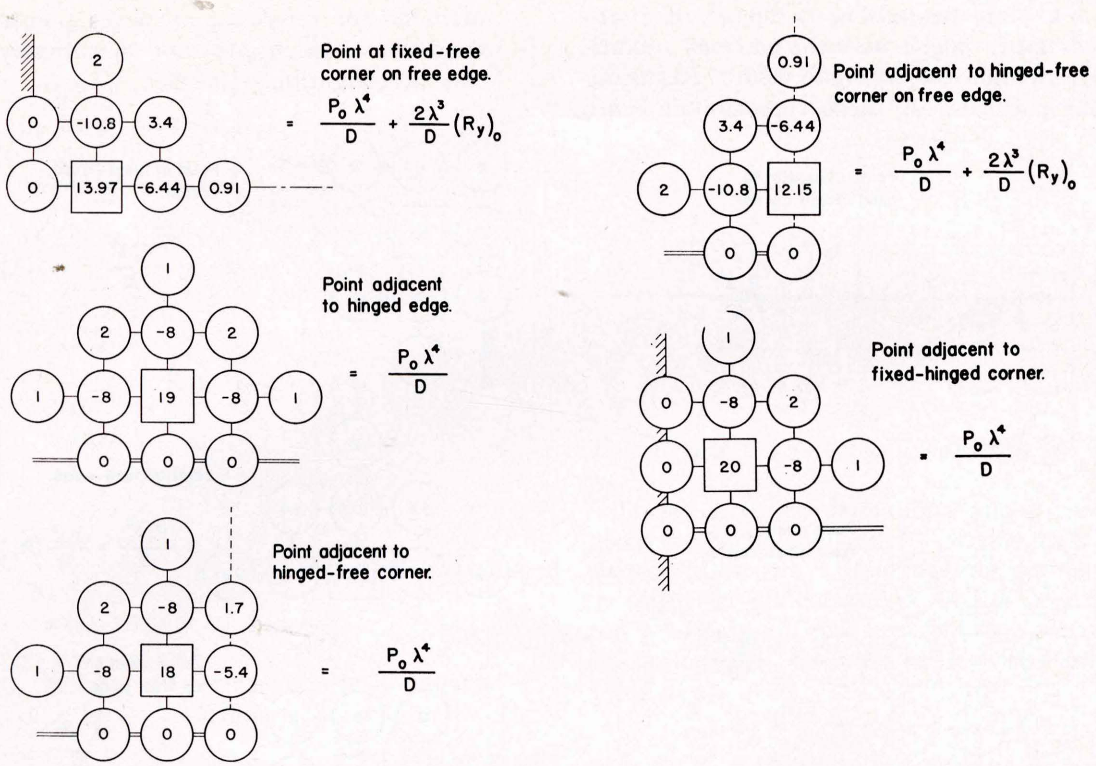

Fig. 3 cont'd. Finite difference equation coefficient patterns for deflection ($\mu = 0.30$).

As stated, the finite difference method usually involves one independent equation for each point that is used as a node point in the superimposed grid. The type of grid used is usually rectangular. It follows that the method must be modified for non-rectangular plates. A method has been presented [17, p. 138] by which the difference equations may be adjusted at irregular edges, but such a method is tedious. It has been applied to skew slabs [5, 10] using oblique coordinates. Since the loading approached zero at the sloping edge, it was convenient to assume the plate rectangular (figure 4). This simplification greatly facilitated the application of the finite difference method in that the theoretical plate was then rectangular (actually square in this case) instead of trapezoidal. It was found that results from this simplified plate varied little from those obtained by a more refined consideration of the sloping edge involving the double Laplacian form of the plate equation.

An infinite number of grid patterns may be superimposed on a plate. The smaller the grid spacing used, the greater will be the number of simultaneous equations obtained, and the more closely their solutions should approximate that of a rigorous mathematical solution of the differential equation. Solutions were desired for sets of equations resulting from the application of the finite difference method to grids of 2 x 2, 3 x 3, 4 x 4, 5 x 5, 6 x 6, and 7 x 7 as shown in figures 5 to 10. It was decided that a comparison of solutions for these sets of equations with experimental results would give an indication of the size of grid that must be used on a thin plate of specified proportion to obtain reasonable predictions of structural behavior. The equations corresponding to the different grid spacings follow:

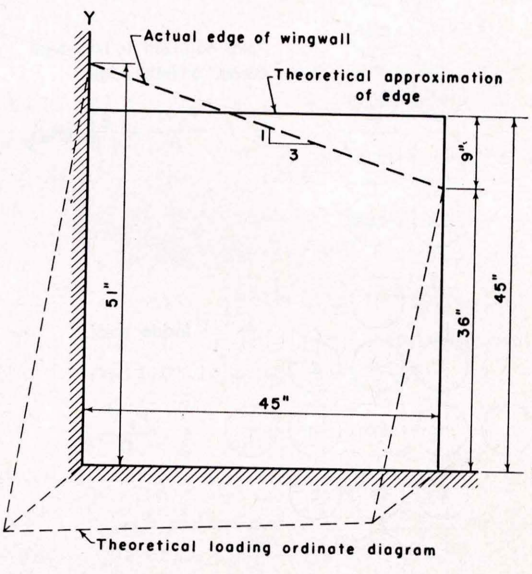

Fig. 4. Theoretical approximation of sloping edge.

Node	Equation	
2x2		
11	$20w_{11} - 5.4w_{12} - 5.4w_{21} + 1.4w_{22}$	$= 14.00000$
12	$-10.8w_{11} + 3.4w_{21} - 4.62w_{22} + 13.06w_{12}$	$= 9.00000$
21	$-10.8w_{11} + 3.4w_{12} - 4.62w_{22} + 13.06w_{21}$	$= 0.00000$
22	$9.24w_{22} - 9.24w_{12} - 9.24w_{21} + 5.6w_{11}$	$= 0.00000$

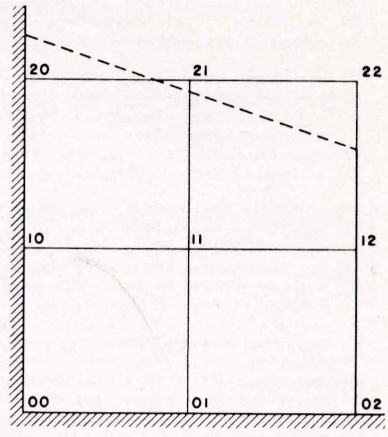

Fig. 5. Node notation for 2 x 2 grid.

Node	Equation	
3x3		
11	$22w_{11} - 8w_{12} + w_{13} - 8w_{21} + 2w_{22} + w_{31}$	$= 0.69695$
12	$-8w_{11} + 20w_{12} - 5.4w_{13} + 2w_{21} - 8w_{22} + 1.7w_{23} + w_{32}$	$= 0.58454$
13	$2w_{11} - 10.8w_{12} + 13.97w_{13} + 3.4w_{22} - 6.44w_{23} + 0.91w_{33}$	$= 0.47213$
21	$-8w_{11} + 2w_{12} + 20w_{21} - 8w_{22} + w_{23} - 5.4w_{31} + 1.7w_{32}$	$= 0.35972$
22	$2w_{11} - 8w_{12} + 1.7w_{13} - 8w_{21} + 18w_{22} - 5.4w_{23} + 1.7w_{31} - 5.4w_{32} + 1.4w_{33}$	$= 0.24731$
23	$3.4w_{12} - 6.44w_{13} + 2w_{21} - 10.8w_{22} + 12.15w_{23} + 3.4w_{32} - 4.62w_{33}$	$= 0.13489$
31	$-10.8w_{21} + 3.4w_{22} + 13.97w_{31} - 6.44w_{32} + 0.91w_{33}$	$= 0.02248$
32	$2w_{12} + 3.4w_{21} - 10.8w_{22} + 3.4w_{23} - 6.44w_{31} + 12.15w_{32} - 4.62w_{33}$	$= 0.00000$
33	$1.82w_{13} + 5.6w_{22} - 9.24w_{23} + 1.82w_{31} + 9.24w_{33}$	$= 0.00000$

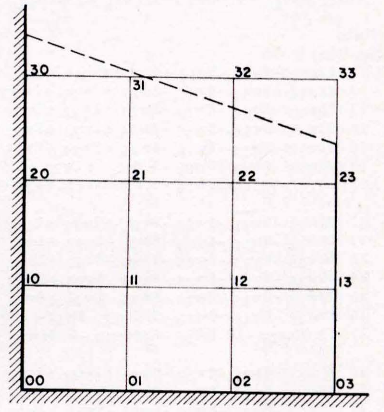

Fig. 6. Node notation for 3 x 3 grid.

Node	Equation	
4x4		
11	$22w_{11} - 8w_{12} + w_{13} - 8w_{21} + 2w_{22} + w_{31}$	$= 0.25609$
12	$-8w_{11} + 21w_{12} - 8w_{13} + w_{14} + 2w_{21} - 8w_{22} + 2w_{23} + w_{32}$	$= 0.22941$
13	$w_{11} - 8w_{12} + 20w_{13} - 5.4w_{14} + 2w_{22} - 8w_{23} + 1.7w_{24} + w_{33}$	$= 0.20273$
14	$2w_{12} - 10.8w_{13} + 13.97w_{14} + 3.4w_{23} - 6.44w_{24} + 0.91w_{34}$	$= 0.17606$
21	$-8w_{11} + 2w_{12} + 21w_{21} - 8w_{22} + w_{23} - 8w_{31} + 2w_{32} + w_{41}$	$= 0.17606$
22	$2w_{11} - 8w_{12} + 2w_{13} - 8w_{21} + 20w_{22} - 8w_{23} + w_{24} + 2w_{31} - 8w_{32} + 2w_{33} + w_{43}$	$= 0.14938$
23	$2w_{12} - 8w_{13} + 1.7w_{14} + w_{21} - 8w_{22} + 19w_{23} - 5.4w_{24} + 2w_{32} - 8w_{33} + 1.7w_{34} + w_{43}$	$= 0.12271$
24	$3.4w_{13} - 6.44w_{14} + 2w_{22} - 10.8w_{23} + 13.06w_{24} + 3.4w_{33} - 6.44w_{41} + 0.91w_{44}$	$= 0.09603$
31	$w_{11} - 8w_{21} + 2w_{22} + 20w_{31} - 8w_{32} + w_{33} - 5.4w_{41} + 1.7w_{42}$	$= 0.09603$
32	$w_{12} + 2w_{21} - 8w_{22} + 2w_{23} - 8w_{31} + 19w_{32} - 8w_{33} + w_{34} + 1.7w_{41} - 5.4w_{42} + 1.7w_{43}$	$= 0.06936$
33	$w_{13} + 2w_{22} - 8w_{23} + 1.7w_{24} + w_{31} - 8w_{32} + 18w_{33} - 5.4w_{34} + 1.7w_{42} - 5.4w_{43} + 1.4w_{44}$	$= 0.04268$
34	$0.91w_{14} + 3.4w_{23} - 6.44w_{24} + 2w_{32} - 10.8w_{33} + 12.15w_{34} + 3.4w_{43} - 4.62w_{44}$	$= 0.01601$
41	$2w_{21} - 10.8w_{31} + 3.4w_{32} + 13.97w_{41} - 6.44w_{42} + 0.91w_{43}$	$= 0.01601$
42	$2w_{22} + 3.4w_{31} - 10.8w_{32} + 3.4w_{33} - 6.44w_{41} + 13.06w_{42} - 6.44w_{43} + 0.91w_{44}$	$= 0.00000$
43	$2w_{23} + 3.4w_{32} - 10.8w_{33} + 3.4w_{34} + 0.91w_{41} - 6.44w_{42} + 12.15w_{43} - 4.62w_{44}$	$= 0.00000$
44	$1.82w_{24} + 5.6w_{33} - 9.24w_{34} + 1.82w_{42} - 9.24w_{43} + 9.24w_{44}$	$= 0.00000$

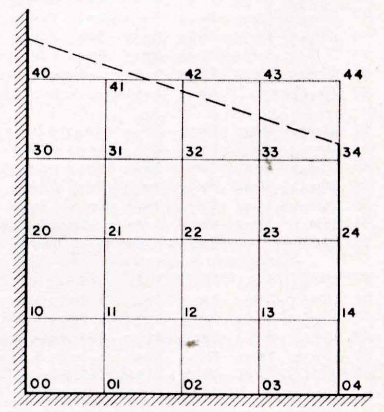

Fig. 7. Node notation for 4 x 4 grid.

Node	Equation	
5x5		
11	$22w_{11} - 8w_{12} + w_{13} - 8w_{21} + 2w_{22} + w_{31}$	$= 0.11363$
12	$-8w_{11} + 21w_{12} - 8w_{13} + w_{14} + 2w_{21} - 8w_{22} + 2w_{23} + w_{32}$	$= 0.10489$
13	$w_{11} - 8w_{12} + 21w_{13} - 8w_{14} + w_{15} + 2w_{22} - 8w_{23} + 2w_{24} + w_{33}$	$= 0.09615$
14	$w_{12} - 8w_{13} + 20w_{14} - 5.4w_{15} + 2w_{23} - 8w_{24} + 1.7w_{25} + w_{34}$	$= 0.08741$
15	$2w_{13} - 10.8w_{14} + 13.97w_{15} + 3.4w_{24} - 6.44w_{25} + 0.91w_{35}$	$= 0.07867$
21	$-8w_{11} + 2w_{12} + 21w_{21} - 8w_{22} + w_{23} - 8w_{31} + 2w_{32} + w_{41}$	$= 0.08741$
22	$2w_{11} - 8w_{12} + 2w_{13} - 8w_{21} + 20w_{22} - 8w_{23} + w_{24} + 2w_{31} - 8w_{32} + 2w_{34} + w_{42}$	$= 0.07867$
23	$2w_{12} - 8w_{13} + 2w_{14} + w_{21} - 8w_{22} + 20w_{23} - 8w_{24} + w_{25} + 2w_{32} - 8w_{33} + 2w_{34} + w_{43}$	$= 0.06993$
24	$2w_{13} - 8w_{14} + 1.7w_{15} + w_{22} - 8w_{23} + 19w_{24} - 5.4w_{25} + 2w_{33} - 8w_{34} + 1.7w_{35} + w_{44}$	$= 0.06119$
25	$3.4w_{14} - 6.44w_{15} + 2w_{23} - 10.8w_{24} + 13.06w_{25} + 3.4w_{34} - 6.44w_{35} + 0.91w_{45}$	$= 0.05245$
31	$w_{11} - 8w_{21} + 2w_{22} + 21w_{31} - 8w_{32} + w_{33} - 8w_{41} + 2w_{42} + w_{51}$	$= 0.06119$
32	$w_{12} + 2w_{21} - 8w_{22} + 2w_{23} - 8w_{31} + 20w_{32} - 8w_{33} + w_{34} + 2w_{41} - 8w_{42} + 2w_{43} + w_{52}$	$= 0.05245$
33	$w_{13} + 2w_{22} - 8w_{23} + 2w_{24} + w_{31} - 8w_{32} + 20w_{33} - 8w_{34} + w_{35} + 2w_{42} - 8w_{43} + 2w_{44} + w_{53}$	$= 0.04371$
34	$w_{14} + 2w_{23} - 8w_{24} + 1.7w_{25} + w_{32} - 8w_{33} + 19w_{34} - 5.4w_{35} + 2w_{43} - 8w_{44} + 1.7w_{45} + w_{54}$	$= 0.03496$
35	$0.91w_{15} + 3.4w_{24} - 6.44w_{25} + 2w_{33} - 10.8w_{34} + 13.06w_{35} + 3.4w_{44} - 6.44w_{45} + 0.91w_{55}$	$= 0.02622$
41	$w_{21} - 8w_{31} + 2w_{32} + 20w_{41} - 8w_{42} + w_{43} - 5.4w_{51} + 1.7w_{52}$	$= 0.03496$
42	$w_{22} + 2w_{31} - 8w_{32} + 2w_{33} - 8w_{41} + 19w_{42} - 8w_{43} + w_{44} + 1.7w_{51} - 5.4w_{52} + 1.7w_{53}$	$= 0.02622$
43	$w_{23} + 2w_{32} - 8w_{33} + 2w_{34} + w_{41} - 8w_{42} + 19w_{43} - 8w_{44} + w_{45} + 1.7w_{52} - 5.4w_{53} + 1.7w_{54}$	$= 0.01748$
44	$w_{24} + 2w_{33} - 8w_{34} + 1.7w_{35} + w_{42} - 8w_{43} + 18w_{44} - 5.4w_{45} + 1.7w_{53} - 5.4w_{54} + 1.4w_{55}$	$= 0.00874$
45	$0.91w_{25} + 3.4w_{34} - 6.44w_{35} + 2w_{43} - 10.8w_{44} + 12.15w_{45} + 3.4w_{54} - 4.62w_{55}$	$= 0.00000$
51	$2w_{31} - 10.8w_{41} + 3.4w_{42} + 13.97w_{51} - 6.44w_{52} + 0.91w_{53}$	$= 0.00874$
52	$2w_{32} + 3.4w_{41} - 10.8w_{42} + 3.4w_{43} - 6.44w_{51} + 13.06w_{52} - 6.44w_{53} + 0.91w_{54}$	$= 0.00000$
53	$2w_{33} + 3.4w_{42} - 10.8w_{43} + 3.4w_{44} + 0.91w_{51} - 6.44w_{52} + 13.06w_{53} - 6.44w_{54} + 0.91w_{55}$	$= 0.00000$
54	$2w_{34} + 3.4w_{43} - 10.8w_{44} + 3.4w_{45} + 0.91w_{52} - 6.44w_{53} + 12.15w_{54} - 4.62w_{55}$	$= 0.00000$
55	$1.82w_{35} + 5.6w_{44} - 9.24w_{45} + 1.82w_{53} - 9.24w_{54} + 9.24w_{55}$	$= 0.00000$

Node	Equation	
6x6		
11	$22w_{11} - 8w_{12} + w_{13} - 8w_{21} + 2w_{22} + w_{31}$	$= 0.05761$
12	$-8w_{11} + 21w_{12} - 8w_{13} + w_{14} + 2w_{21} - 8w_{22} + 2w_{23} + w_{32}$	$= 0.05409$
13	$w_{11} - 8w_{12} + 21w_{13} - 8w_{14} + w_{15} + 2w_{22} - 8w_{23} + 2w_{24} + w_{33}$	$= 0.05058$
14	$w_{12} - 8w_{13} + 21w_{14} - 8w_{15} + w_{16} + 2w_{23} - 8w_{24} + 2w_{25} + w_{34}$	$= 0.04707$
15	$w_{13} - 8w_{14} + 20w_{15} - 5.4w_{16} + 2w_{24} - 8w_{25} + 1.7w_{26} + w_{35}$	$= 0.04356$
16	$2w_{14} - 10.8w_{15} + 13.97w_{16} + 3.4w_{25} - 6.44w_{26} + 0.91w_{36}$	$= 0.04005$

21	$-8w_{11} + 2w_{12} + 21w_{21} - 8w_{22} + w_{23} - 8w_{31} + 2w_{32} + w_{41}$	$= 0.04707$
22	$2w_{11} - 8w_{12} + 2w_{13} - 8w_{21} + 20w_{22} - 8w_{23} + w_{24} + 2w_{31} - 8w_{32} + 2w_{33} + w_{42}$	$= 0.04356$
23	$2w_{12} - 8w_{13} + 2w_{14} + w_{21} - 8w_{22} + 20w_{23} - 8w_{24} + w_{25} + 2w_{32} - 8w_{33} + 2w_{34} + w_{43}$	$= 0.04005$
24	$2w_{13} - 8w_{14} + 2w_{15} + w_{22} - 8w_{23} + 20w_{24} - 8w_{25} + w_{26} + 2w_{33} - 8w_{34} + 2w_{35} + w_{44}$	$= 0.03653$
25	$2w_{14} - 8w_{15} + 1.7w_{16} + w_{23} - 8w_{24} + 19w_{25} - 5.4w_{26} + 2w_{34} - 8w_{35} + 1.7w_{36} + w_{45}$	$= 0.03302$
26	$3.4w_{15} - 6.44w_{16} + 2w_{24} - 10.8w_{25} + 13.06w_{26} + 3.4w_{35} - 6.44w_{36} + 0.91w_{46}$	$= 0.02951$
31	$w_{11} - 8w_{21} + 2w_{22} + 21w_{31} - 8w_{32} + w_{33} - 8w_{41} + 2w_{42} + w_{51}$	$= 0.03653$
32	$w_{12} + 2w_{21} - 8w_{22} + 2w_{23} - 8w_{31} + 20w_{32} - 8w_{33} + w_{34} + 2w_{41} - 8w_{42} + 2w_{43} + w_{52}$	$= 0.03302$
33	$w_{13} + 2w_{22} - 8w_{23} + 2w_{24} + w_{31} - 8w_{32} + 20w_{33} - 8w_{34} + w_{35} + 2w_{42} - 8w_{43} + 2w_{44} + w_{53}$	$= 0.02951$
34	$w_{14} + 2w_{23} - 8w_{24} + 2w_{25} + w_{32} - 8w_{33} + 20w_{34} - 8w_{35} + w_{36} + 2w_{43} - 8w_{44} + 2w_{45} + w_{54}$	$= 0.02599$
35	$w_{15} + 2w_{24} - 8w_{25} + 1.7w_{26} + w_{33} - 8w_{34} + 19w_{35} - 5.4w_{36} + 2w_{44} - 8w_{45} + 1.7w_{46} + w_{55}$	$= 0.02248$
36	$0.91w_{16} + 3.4w_{25} - 6.44w_{26} + 2w_{34} - 10.8w_{35} + 13.06w_{36} + 3.4w_{45} - 6.44w_{46} + 0.91w_{56}$	$= 0.01897$
41	$w_{21} - 8w_{31} + 2w_{32} + 21w_{41} - 8w_{42} + w_{43} - 8w_{51} + 2w_{52} + w_{61}$	$= 0.02599$
42	$w_{22} + 2w_{31} - 8w_{32} + 2w_{33} - 8w_{41} + 20w_{42} - 8w_{43} + w_{44} + 2w_{51} - 8w_{52} + 2w_{53} + w_{62}$	$= 0.02248$
43	$w_{23} + 2w_{32} - 8w_{33} + 2w_{34} + w_{41} - 8w_{42} + 20w_{43} - 8w_{44} + w_{45} + 2w_{52} - 8w_{53} + 2w_{54} + w_{63}$	$= 0.01897$
44	$w_{24} + 2w_{33} - 8w_{34} + 2w_{35} + w_{42} - 8w_{43} + 20w_{44} - 8w_{45} + w_{46} + 2w_{53} - 8w_{54} + 2w_{55} + w_{64}$	$= 0.01546$
45	$w_{25} + 2w_{34} - 8w_{35} + 1.7w_{36} + w_{43} - 8w_{44} + 19w_{45} - 5.4w_{46} + 2w_{54} - 8w_{55} + 1.7w_{56} + w_{65}$	$= 0.11194$
46	$0.91w_{26} + 3.4w_{35} - 6.44w_{36} + 2w_{44} - 10.8w_{45} + 13.06w_{46} + 3.4w_{55} - 6.44w_{56} + 0.91w_{66}$	$= 0.00843$
51	$w_{31} - 8w_{41} + 2w_{42} + 20w_{51} - 8w_{52} + w_{53} - 5.4w_{61} + 1.7w_{62}$	$= 0.01546$
52	$w_{32} + 2w_{41} - 8w_{42} + 2w_{43} - 8w_{51} + 19w_{52} - 8w_{53} + w_{54} + 1.7w_{61} - 5.4w_{62} + 1.7w_{63}$	$= 0.01194$
53	$w_{33} + 2w_{42} - 8w_{43} + 2w_{44} + w_{51} - 8w_{52} + 19w_{53} - 8w_{54} + w_{55} + 1.7w_{62} - 5.4w_{63} + 1.7w_{64}$	$= 0.00843$
54	$w_{34} + 2w_{43} - 8w_{44} + 2w_{45} + w_{52} - 8w_{53} + 19w_{54} - 8w_{55} + w_{56} + 1.7w_{63} - 5.4w_{64} + 1.7w_{65}$	$= 0.00492$
55	$w_{35} + 2w_{44} - 8w_{45} + 1.7w_{46} + w_{53} - 8w_{54} + 18w_{55} - 5.4w_{56} + 1.7w_{64} - 5.4w_{65} + 1.4w_{66}$	$= 0.00141$
56	$0.91w_{36} + 3.4w_{45} - 6.44w_{46} + 2w_{54} - 10.8w_{55} + 12.15w_{56} + 3.4w_{65} - 4.62w_{66}$	$= 0.00000$
61	$2w_{41} - 10.8w_{51} + 3.4w_{52} + 13.97w_{61} - 6.44w_{62} + 0.91w_{63}$	$= 0.00492$
62	$2w_{42} + 3.4w_{51} - 10.8w_{52} + 3.4w_{53} - 6.44w_{61} + 13.06w_{62} - 6.44w_{63} + 0.91w_{64}$	$= 0.00141$
63	$2w_{43} + 3.4w_{52} - 10.8w_{53} + 3.4w_{54} + 0.91w_{61} - 6.44w_{62} + 13.06w_{63} - 6.44w_{64} + 0.91w_{65}$	$= 0.00000$
64	$2w_{44} + 3.4w_{53} - 10.8w_{54} + 3.4w_{55} + 0.91w_{62} - 6.44w_{63} + 13.06w_{64} - 6.44w_{65} + 0.91w_{66}$	$= 0.00000$
65	$2w_{45} + 3.4w_{54} - 10.8w_{55} + 3.4w_{56} + 0.91w_{63} - 6.44w_{64} + 12.15w_{65} - 4.62w_{66}$	$= 0.00000$
66	$1.82w_{46} + 5.6w_{55} - 9.24w_{56} + 1.82w_{64} - 9.24w_{65} + 9.24w_{66}$	$= 0.00000$

Node 7 x 7	Equation	
11	$22w_{11} - 8w_{21} - 8w_{12} + w_{13} + w_{31} + 2w_{22}$	$= 0.03218$
12	$21w_{12} - 8w_{11} - 8w_{13} - 8w_{22} + 2w_{21} + 2w_{23} + w_{32} + w_{14}$	$= 0.03055$
13	$21w_{13} - 8w_{12} - 8w_{14} - 8w_{23} + 2w_{22} + 2w_{24} + w_{35} + w_{15} + w_{11}$	$= 0.02893$
14	$21w_{14} - 8w_{13} - 8w_{15} - 8w_{24} + 2w_{23} + 2w_{23} + w_{34} + w_{16} + w_{12}$	$= 0.02730$
15	$21w_{15} - 8w_{14} - 8w_{16} - 8w_{25} + 2w_{24} + 2w_{26} + w_{35} + w_{17} + w_{13}$	$= 0.02568$
16	$20w_{16} - 8w_{15} - 8w_{26} - 5.4w_{17} + 2w_{25} + 1.7w_{27} + w_{14} + w_{36}$	$= 0.02406$
17	$13.97w_{17} - 10.8w_{16} - 6.44w_{27} + 3.4w_{26} + 2w_{15} + 0.91w_{37}$	$= 0.02243$
21	$21w_{21} - 8w_{11} - 8w_{22} - 8w_{31} + 2w_{12} + 2w_{32} + w_{41} + w_{23}$	$= 0.02730$
22	$20w_{22} - 8w_{12} - 8w_{23} - 8w_{21} - 8w_{32} + 2w_{11} + 2w_{13} + 2w_{33} + 2w_{31} + w_{42} + w_{24}$	$= 0.02568$
23	$20w_{23} - 8w_{13} - 8w_{24} - 8w_{33} - 8w_{22} + 2w_{12} + 2w_{14} + 2w_{34} + 2w_{32} + w_{25} + w_{43} + w_{21}$	$= 0.02406$
24	$20w_{24} - 8w_{14} - 8w_{25} - 8w_{34} - 8w_{23} + 2w_{13} + 2w_{15} + 2w_{35} + 2w_{33} + w_{26} + w_{44} + w_{22}$	$= 0.02243$
25	$20w_{25} - 8w_{15} - 8w_{26} - 8w_{35} - 8w_{24} + 2w_{14} + 2w_{16} + 2w_{36} + 2w_{34} + w_{27} + w_{45} + w_{23}$	$= 0.02081$
26	$19w_{26} - 8w_{16} - 8w_{25} - 5.4w_{27} - 8w_{36} + 2w_{15} + 2w_{35} + 1.7w_{37} + w_{24} + w_{46}$	$= 0.01918$
27	$13.06w_{27} - 10.8w_{26} - 6.44w_{17} - 6.44w_{37} + 3.4w_{16} + 3.4w_{36} + 0.91w_{47} + 2w_{25}$	$= 0.01755$
31	$21w_{31} - 8w_{21} - 8w_{32} - 8w_{41} + 2w_{22} + 2w_{42} + w_{51} + w_{33} + w_{11}$	$= 0.02243$
32	$20w_{32} - 8w_{22} - 8w_{33} - 8w_{31} - 8w_{42} + 2w_{21} + 2w_{23} + 2w_{43} + 2w_{41} + w_{52} + w_{34} + w_{12}$	$= 0.02080$
33	$20w_{33} - 8w_{23} - 8w_{34} - 8w_{43} - 8w_{32} + 2w_{22} + 2w_{24} + 2w_{44} + 2w_{42} + w_{35} + w_{53} + w_{13}$	$= 0.01918$
34	$20w_{34} - 8w_{24} - 8w_{35} - 8w_{44} - 8w_{33} + 2w_{23} + 2w_{25} + 2w_{45} + 2w_{43} + w_{36} + w_{54} + w_{32} + w_{14}$	$= 0.01755$
35	$20w_{35} - 8w_{25} - 8w_{37} - 8w_{45} - 9w_{34} + 2w_{24} + 2w_{26} + 2w_{46} + 2w_{44} + w_{37} + w_{55} + w_{33} + w_{15}$	$= 0.01593$
36	$19w_{36} - 8w_{26} - 8w_{35} - 5.4w_{37} - 8w_{46} + 2w_{25} + 2w_{45} + 1.7w_{47} + w_{34} + w_{36} + 1.7w_{27} + w_{16}$	$= 0.01430$
37	$13.06w_{37} - 10.8w_{36} - 6.44w_{27} - 6.44w_{47} + 3.4w_{26} + 3.4w_{46} + 0.91w_{57} + 0.91w_{17} + 2w_{35}$	$= 0.01268$
41	$21w_{41} - 8w_{31} - 8w_{42} - 8w_{51} + 2w_{32} + 2w_{52} + w_{61} + w_{43} + w_{21}$	$= 0.01755$
42	$20w_{42} - 8w_{32} - 8w_{43} - 8w_{41} - 8w_{52} + 2w_{31} + 2w_{33} + 2w_{53} + 2w_{51} + w_{62} + w_{44} + w_{22}$	$= 0.01592$
43	$20w_{43} - 8w_{33} - 8w_{44} - 8w_{53} - 8w_{42} + 2w_{32} + 2w_{34} + 2w_{54} - 2w_{52} + w_{45} + w_{63} + w_{41} + w_{23}$	$= 0.01430$
44	$20w_{44} - 8w_{34} - 8w_{45} - 8w_{54} - 8w_{43} + 2w_{33} + 2w_{35} + 2w_{55} + 2w_{53} + w_{46} + w_{64} + w_{42} + w_{24}$	$= 0.01268$
45	$20w_{45} - 8w_{35} - 8w_{46} - 8w_{55} - 8w_{44} + 2w_{34} + 2w_{36} + 2w_{56} + 2w_{54} + w_{47} + w_{65} + w_{43} + w_{25}$	$= 0.01105$
46	$19w_{46} - 8w_{36} - 8w_{45} - 5.4w_{47} - 8w_{56} + 2w_{35} + 2w_{55} + 1.7w_{57} + w_{44} + w_{66} + w_{26} + 1.7w_{37}$	$= 0.00943$
47	$13.06w_{47} - 10.8w_{46} - 6.44w_{37} - 6.44w_{57} + 3.4w_{36} + 3.4w_{56} + 0.91w_{67} + 0.91w_{27} + 2w_{45}$	$= 0.00780$
51	$21w_{51} - 8w_{41} - 8w_{52} - 8w_{61} + 2w_{42} + 2w_{62} + w_{71} + w_{53} + w_{31}$	$= 0.01268$
52	$20w_{52} - 8w_{42} - 8w_{53} - 8w_{51} - 8w_{62} + 2w_{41} + 2w_{43} + 2w_{63} + 2w_{61} + w_{72} + w_{54} + w_{32}$	$= 0.01105$
53	$20w_{53} - 8w_{43} - 8w_{54} - 8w_{63} - 8w_{52} + 2w_{42} + 2w_{44} + 2w_{64} + 2w_{62} + w_{55} + w_{73} + w_{51} + w_{33}$	$= 0.00943$
54	$20w_{54} - 8w_{44} - 8w_{55} - 8w_{64} - 8w_{53} + 2w_{43} + 2w_{45} + 2w_{65} + w_{56} + w_{74} + w_{52} + w_{34}$	$= 0.00780$
55	$20w_{55} - 8w_{45} - 8w_{56} - 8w_{65} - 8w_{54} + 2w_{44} + 2w_{46} + 2w_{66} + 2w_{64} + w_{57} + w_{75} + w_{53} + w_{35}$	$= 0.00618$
56	$19w_{56} - 8w_{46} - 8w_{55} - 5.4w_{57} - 8w_{66} + 2w_{45} + 2w_{65} + 1.7w_{67} + w_{54} + w_{76} + w_{36} + 1.7w_{47}$	$= 0.00455$
57	$13.06w_{57} - 10.8w_{46} - 6.44w_{37} - 6.44w_{57} + 3.4w_{36} + 3.4w_{56} + 0.91w_{67} + 0.91w_{27} + 2w_{45}$	$= 0.00293$
61	$20w_{61} - 8w_{51} - 8w_{62} - 5.4w_{71} + 2w_{52} + 1.7w_{72} + w_{41} + w_{63}$	$= 0.00781$
62	$19w_{62} - 8w_{52} - 8w_{61} - 8w_{63} - 5.4w_{72} + 2w_{51} + 2w_{53} + 1.7w_{73} + w_{42} + w_{64}$	$= 0.00618$
63	$19w_{63} - 8w_{53} - 8w_{62} - 8w_{64} - 5.4w_{73} + 2w_{52} + 2w_{54} + 1.7w_{72} + 1.7w_{74} + w_{43} + w_{65} + w_{61}$	$= 0.00456$
64	$19w_{64} - 8w_{54} - 8w_{63} - 8w_{65} - 5.4w_{74} + 2w_{53} + 2w_{55} + 1.7w_{73} + 1.7w_{75} + w_{44} + w_{66} + w_{62}$	$= 0.00293$
65	$19w_{65} - 8w_{55} - 8w_{64} - 8w_{66} - 5.4w_{75} + 2w_{54} + 2w_{56} + 1.7w_{74} + 1.7w_{76} + w_{45} + w_{67} + w_{63}$	$= 0.00131$
66	$18w_{66} - 8w_{56} - 8w_{65} - 5.4w_{67} - 5.4w_{76} + 2w_{55} + 1.7w_{57} + 1.7w_{75} + 1.4w_{77} + w_{46} + w_{64}$	$= 0.00000$
67	$12.15w_{67} - 10.8w_{66} - 6.44w_{57} - 4.62w_{77} + 3.4w_{56} + 3.4w_{76} + 2w_{65} + 0.91w_{47}$	$= 0.00000$
71	$13.97w_{71} - 10.8w_{61} - 6.44w_{72} + 3.4w_{62} + 0.91w_{73} + 2w_{51}$	$= 0.00293$
72	$13.06w_{72} - 10.8w_{62} - 6.44w_{71} - 6.44w_{73} + 3.4w_{61} + 3.4w_{63} + 2w_{52} + 0.91w_{74}$	$= 0.00130$
73	$13.06w_{73} - 10.8w_{63} - 6.44w_{72} - 6.44w_{74} + 3.4w_{62} + 3.4w_{64} + 2w_{53} + 0.91w_{75} + 0.91w_{71}$	$= 0.00000$
74	$13.06w_{74} - 10.8w_{64} - 6.44w_{73} - 6.44w_{75} + 3.4w_{63} + 3.4w_{65} + 2w_{54} + 0.91w_{76} + 0.91w_{72}$	$= 0.00000$
75	$13.06w_{75} - 10.8w_{65} - 6.44w_{74} - 6.44w_{76} + 3.4w_{64} + 3.4w_{66} + 2w_{55} + 0.91w_{73} + 0.91w_{77}$	$= 0.00000$
76	$12.15w_{76} - 10.8w_{66} - 6.44w_{75} - 4.62w_{77} + 3.4w_{65} + 3.4w_{67} + 2w_{56} + 0.91w_{74}$	$= 0.00000$
77	$9.24w_{77} - 9.24w_{67} - 9.24w_{76} + 5.6w_{66} + 1.82w_{57} + 1.82w_{75}$	$= 0.00000$

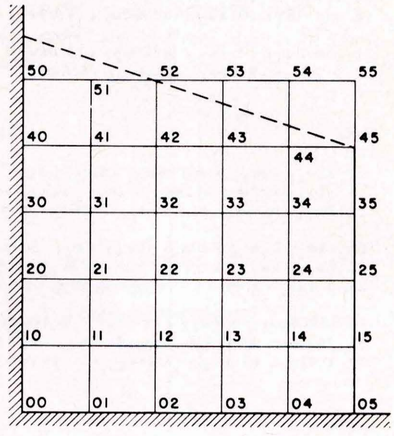

Fig. 8. Node notation for 5 x 5 grid.

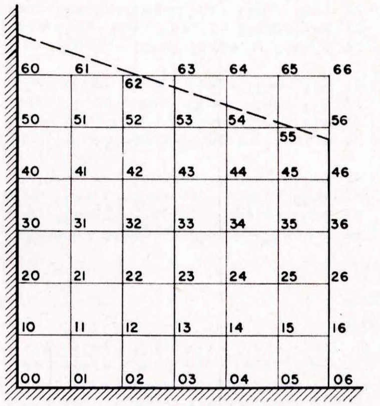

Fig. 9. Node notation for 6 x 6 grid.

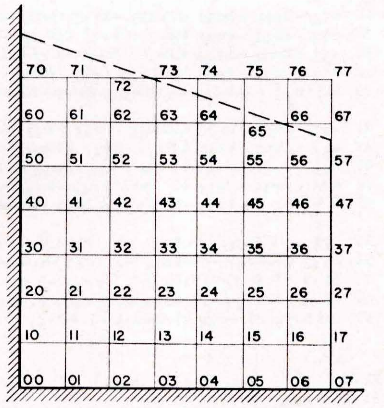

Fig. 10. Node notation for 7 x 7 grid.

The only practical method for solving the simultaneous equations resulting from the finite difference method was that which used high speed digital computers. The sets of sixteen and forty-nine equations were solved by the Gauss-Seidel method on the Navy's Logistics Computer at George Washington University, Washington, D. C. The remaining sets of equations were solved by International Business Machines Corporation, New York, New York, on the Type 650 Drum Calculator. The solutions of all sets of equations are listed in tables I to VI. These values are theoretical deflections at the various node points on the plate under action of a triangularly distributed load corresponding to a maximum load ordinate of $p_f = 2.8498$ psi at the fixed-fixed corner, except for the 2 x 2 grid for which $p_f = 16.678$ psi.

Table I. Solutions to Equations from 2 x 2 Grid.

Node	Solution p_f=16.678 psi
11	1.84560023
12	3.13409361
21	2.20241659
22	4.21796461

Table II. Solutions to Equations from 3 x 3 Grid.

Node	Theoretical[a] p_f=2.8498 psi
11	0.12707355
12	0.23565655
13	0.31949340
21	0.19598481
22	0.40846871
23	0.58251333
31	0.21803188
32	0.49876915
33	0.72784948

[a]Value as received from I. B. M.

Table III. Solutions to Equations from 4 x 4 Grid.

Node	Theoretical[a] p_f=2.8498 psi
11	0.0575381
12	0.1156772
13	0.1585868
14	0.1965613
21	0.1031837
22	0.2300458
23	0.3352344
24	0.4293408
31	0.1224602
32	0.2961565
33	0.4522082
34	0.5897135
41	0.1306534
42	0.3395514
43	0.5349057
44	0.6991052

[a]Value as received from I. B. M. and George Washington University.

Table IV. Solutions to Equations from 5 x 5 Grid.

Node	Theoretical[a] p_f=2.8498 psi
11	0.02948352
12	0.06324810
13	0.08956861
14	0.11056832
15	0.13006897
21	0.05853695
22	0.13753822
23	0.20674564
24	0.26434140
25	0.31944521
31	0.07462719
32	0.18827106
33	0.29639327
34	0.38989986
35	0.47810265
41	0.08154205
42	0.21783206
43	0.35579272
44	0.47806407
45	0.59002736
51	0.08420199
52	0.23977177
53	0.40366937
54	0.54898761
55	0.67559680

[a]Value as received from I. B. M.

The matter of predicting stresses at various node points follows from these deflections rather nicely. The partial differential equations for moments per unit length at a point in a plate are as stated previously [1]:

$$(M_y)_o = -\frac{D}{\lambda^2}\Big[-(2+2\mu)\,w_o + w_N + w_S + \mu\left(w_W + w_E\right)\Big]$$

$$(M_{xy})_o = \frac{D\,(1-\mu)}{4\lambda^2}\left(w_{SE} - w_{NE} - w_{SW} + w_{NW}\right)$$

$$(M_x)_o = -\frac{D}{\lambda^2}\Big[-(2+2\mu)\,w_o + w_W + w_E + \mu\left(w_N + w_S\right)\Big]$$

Table V. Solutions to Equations from 6 x 6 Grid.

Node	Theoretical[a] p_f=2.8498 psi
11	0.01659571
12	0.03762697
13	0.05518299
14	0.06896651
15	0.08115092
16	0.09207324
21	0.03559893
22	0.08739756
23	0.13546017
24	0.17576368
25	0.21111753
26	0.24593091
31	0.04833338
32	0.12624910
33	0.20409736
34	0.27269807
35	0.33361650
36	0.39371353
41	0.05489353
42	0.15090707
43	0.25258180
44	0.34577057
45	0.42943596
46	0.51038656
51	0.05815912
52	0.16652740
53	0.28666490
54	0.39989364
55	0.50177611
56	0.59752615
61	0.05868831
62	0.17867620
63	0.31632693
64	0.44755731
65	0.56405889
66	0.66879237

[a]Value as received from I. B. M.

Table VI. Solutions to Equations from 7 x 7 Grid.

Node	Theoretical[a] p_f=2.8498 psi
11	0.0100122
12	0.0237897
13	0.0360156
14	0.0458019
15	0.0539833
16	0.0617751
17	0.0680694
21	0.0228180
22	0.0580875
23	0.0924476
24	0.1220112
25	0.1473186
26	0.1706095
27	0.1934330
31	0.0325827
32	0.0875554
33	0.1447239
34	0.1964437
35	0.2418685
36	0.2836006
37	0.3256493
41	0.0384426
42	0.1081356
43	0.1844953
44	0.2564201
45	0.3210959
46	0.3806546
47	0.4401452
51	0.0415400
52	0.1212884
53	0.2124635
54	0.3011918
55	0.3824841
56	0.4573243
57	0.5306064
61	0.0433211
62	0.1303344
63	0.2333938
64	0.3362106
65	0.4314696
66	0.5185744
67	0.6016478
71	0.0427700
72	0.1370165
73	0.2521648
74	0.3686247
75	0.4764932
76	0.5733954
77	0.6623876

[a]Value as received from George Washington University.

$$M_x = -D\left(\frac{\partial^2 w}{\partial x^2} + \mu\,\frac{\partial^2 w}{\partial y^2}\right)$$

$$M_y = -D\left(\frac{\partial^2 w}{\partial y^2} + \mu\,\frac{\partial^2 w}{\partial x^2}\right)$$

$$M_{xy} = M_{yx} = D\,(1-\mu)\,\frac{\partial^2 w}{\partial x \partial y}$$

Coefficient patterns for moment at typical points in the plate, similar to those for deflections, are presented in figure 11.

To compute stress from these moment expressions, multiply by the constant $6/h^2$ (reciprocal of section modulus of a rectangular section one inch wide).

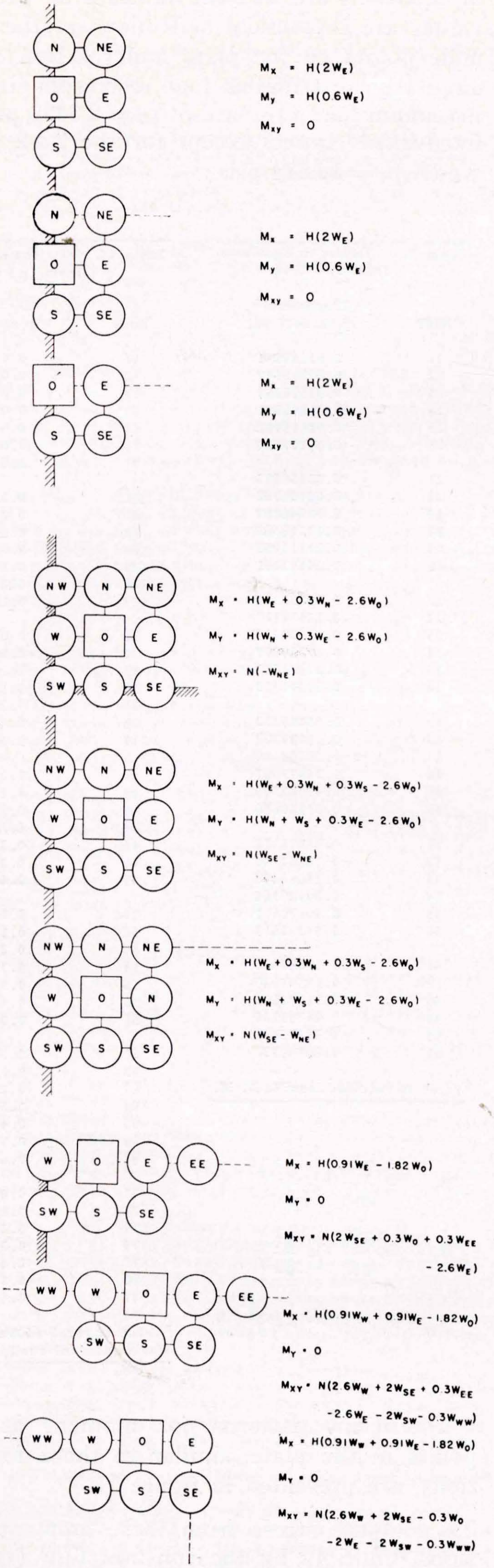

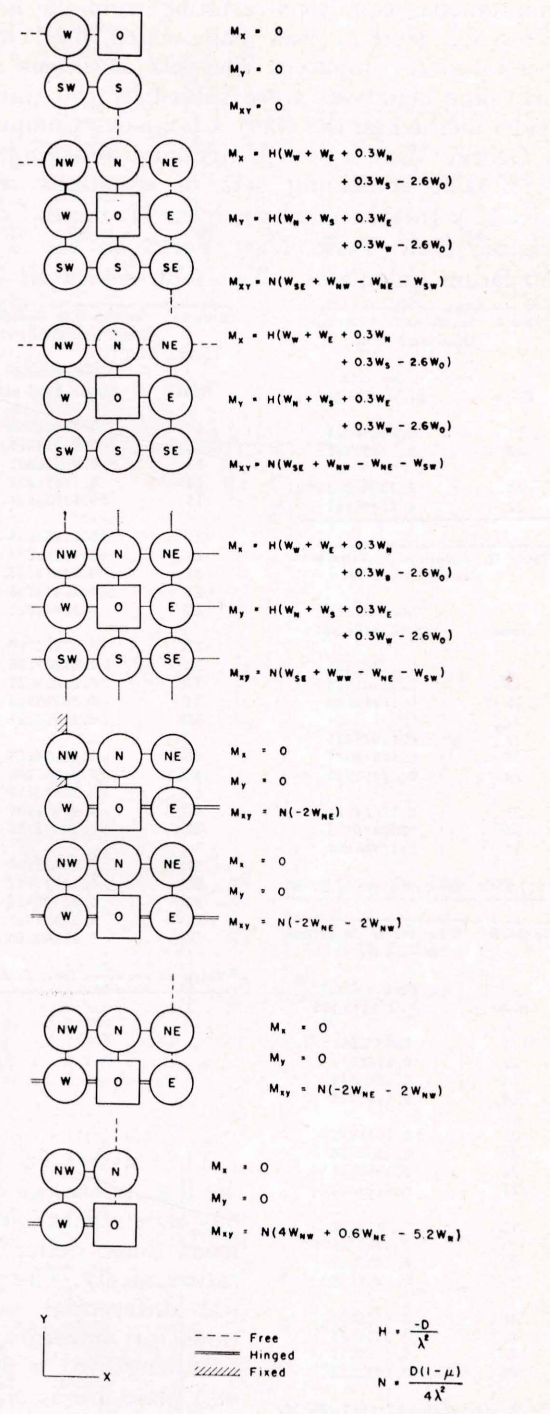

Fig. 11. Finite difference equation patterns for moment ($\mu = 0.3$).

EXPERIMENTAL INVESTIGATION

The experimental investigation was designed to be consistent with the Iowa Highway Commission assumptions of fixation and loads. The investigation was performed on thin trapezoidal aluminum plates 45 in. x 51 in., fixed at two edges and free on the other two. In plan these plates were geometrically similar to the wingwall shown in figure 1. A distributed load varying linearly from zero at the sloping edge to a maximum at the fixed corner was used. Strains and deflections at various points on the plate were measured. Figure 12 shows the test setup.

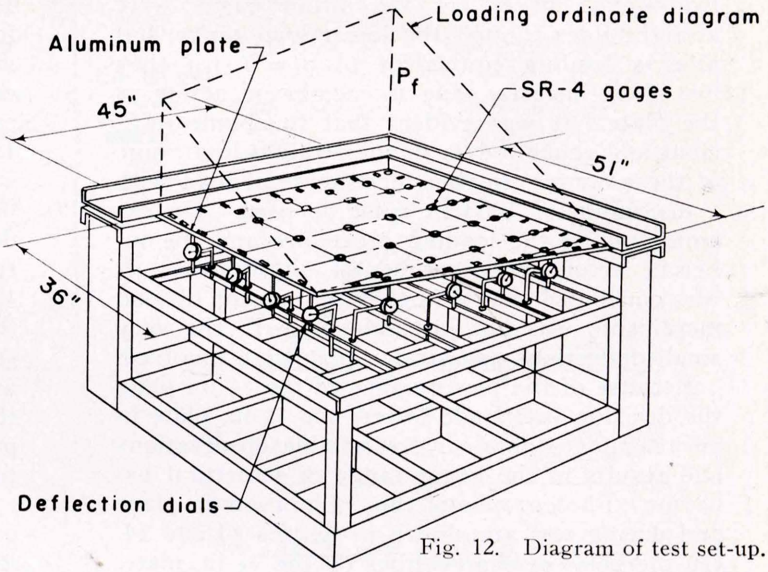

Fig. 12. Diagram of test set-up.

The actual loading was a distributed load simulated by a large number of free-standing concentrated loads, each of which was a combination of small modular weights. The weight sizes were 10 lb, 5 lb, 2 lb, 0.67 lb, and 0.33 lb. The 10 lb and 5 lb units were accomplished by inserting steel shot in one quart cans. The smaller weights were sand-filled plastic bags. By using these modular weights, it was possible to load the plate in six equal increments. The maximum total load was approximately 4,000 lb. It was not feasible to use more than 4,000 lb because of the nature of the loading system and the material used.

Readings at various points on the plate at each increment of load deflection were taken by Federal full jeweled dial indicators with a least count of 0.001 in. and a range of 1 in. Simultaneously, SR-4 resistance type strain gage readings were taken for a number of points. Linear type gages were used at points where directions of principal stresses were assumed to be known, and rosette type gages were used at other points.

The first set of tests was performed on a ¾ in. plate of size and shape previously mentioned. It was found that the deflections and strains even under the maximum load of 4000 lb were too small and erratic to be reliable. To obtain greater deflections and strains under the maximum load of 4,000 lb, ½ in. and ⅜ in. thickness plates of the same overall size (45 in. x 51 in.) were obtained.

The ⅜ in. plate was tested first. The purpose of the test was one of reconnaissance, therefore only a minimum number of gages were used. Load-deflection and load-strain curves for various points on the plate were not linear, and the plate did not return to consistent zero positions even after a series of loading cycles. Nonlinear slippage of the supports was suspected, and an attempt was made to correct this by inserting cement grout between the plate and its channel supports. This grouting procedure solved the problem of support slippage in that the plate consistently returned to its original position after being unloaded, usually within the least count of the deflection dials (0.001 in.). On the basis of this performance, it was decided to gage the plate completely and perform final tests. Approximately 80 SR-4 resistance type strain gages were then applied, and final tests of the plate were commenced using the system of six load increments.

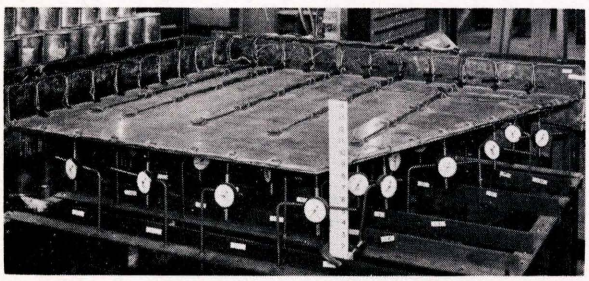

Fig. 13. Plate before loading.

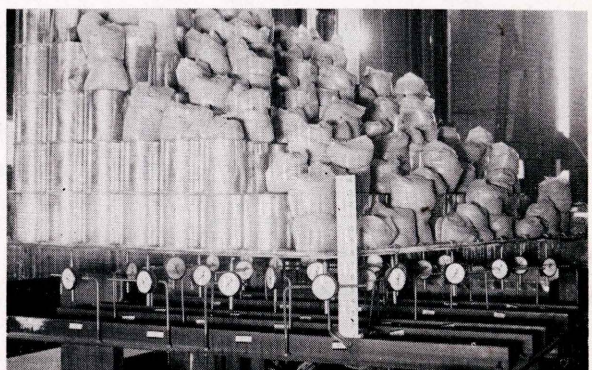

Fig. 14. Plate under maximum load.

Load-deflection curves for the dial gages and load-strain curves for the strain gages were straight lines though the lower load range, but after a loading equivalent to $p_f = 1$ psi they lost their linearity, due to membrane action of the plate. It was evident that to obtain sufficient and reliable data in the straight-line range of these curves, smaller increments of load with a maximum of 1000 lb must be used. On examination of the loading procedure and the inherent errors in experimental observations, it was concluded that a further refinement of load increments was not justifiable due to the very small deflections and strains that were involved.

Because of the performance of the 3/8 in. plate the decision was made to test the 1/2 in. plate in an attempt to obtain more reliable observations and results in the linear range of structural behavior. Photographs of this 1/2 in. plate in place and during test are shown in figures 13 and 14. On the basis of observations on the 3/8 in. plate, more complete gaging was accomplished in certain areas where previous data were weak. This more complete gaging resulted in a total of 25 dial gages and 118 SR-4 strain gages, the locations of which may be seen in figures 15 and 16.

Three complete tests were performed on the 1/2 in. plate, each test involving six equal increments of load up to approximately 4000 lb total weight. The load was removed and final readings with zero load on the plate were taken immediately after the maximum load was applied in each of the three tests. The majority of the deflection dial readings before and after test agreed within the least count of the dial (0.001 in.); the maximum deviation observed at the outside corner, was 0.004 in. out of a maximum deflection of 0.668 in.

Load-deflection curves for each dial indicator and load-strain curves for each strain gage were then drawn for each of the three tests. It was found that the load deflection curves for each test were almost identical, but load-strain curves did not agree as closely, due to the exceedingly small strains involved (in many cases less than the least count of the M-unit). It was therefore decided that the best overall strain gage results could be obtained by averaging the data from the three tests. Sample load-deflection and load Ee (modulus of elasticity times unit strain) curves are shown in figures 17 and 18. The linearity of both sets of curves throughout the loading sequence is evident. The slopes of these curves are respectively deflection and Ee for a load corresponding to $p_f = 1$ psi at the fixed corner. The resultant slopes of all experimental curves are in table VII. The notation used is shown in figures 15 and 16.

As a further check on the consistency of the experimental observations, figures 19 to 22 show deflection sections and Ee sections for each corresponding grid line on the plate. In drawing these curves, the slopes previously evaluated were used as ordinates. With the deflection and Ee sections established, it was possible to construct deflection and Ee contour diagrams or charts for the 1/2 in. plate subjected to a triangular loading equivalent to $p_f = 1$ psi. The uniformity of these contour charts, reductions or

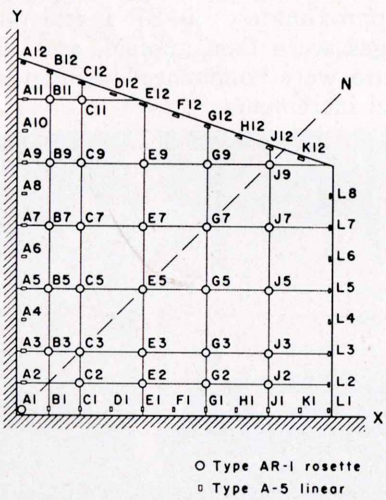

Fig. 15. Location of deflection dial gages.

Table VII. Slopes of load-deflection curves.

Point of 5x5 Grid	Slope (in. /p_f)	Point of 5x5 Grid	Slope (in. /p_f)
11	0.0085	41	0.0281
12	0.0191	42	0.0716
13	0.0275	43	0.1203
14	0.0347	44	0.1654
15	0.0401	45	0.2016
21	0.0183	51	0.0252
22	0.0445	52	0.0725
23	0.0685	E1	0.0217
24	0.0873	E3	0.1300
25	0.1054	E4	0.1724
31	0.0247		
32	0.0624		
33	0.0995		
34	0.1316		
35	0.1595		

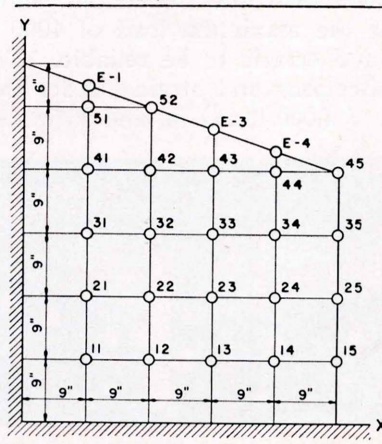

Fig. 16. Location of SR-4 gages.

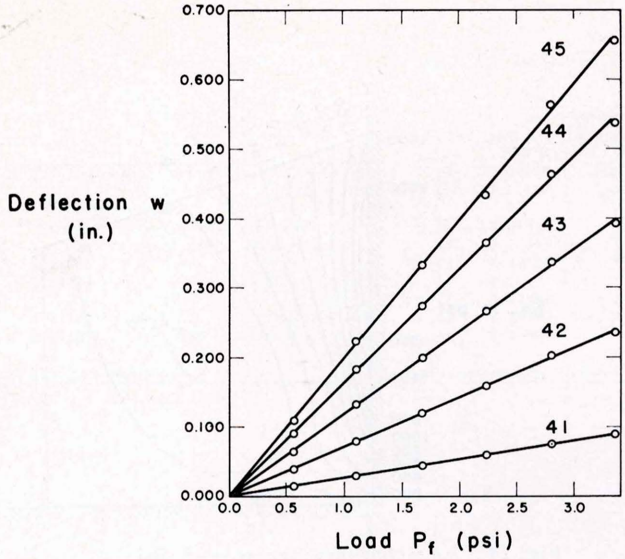

Fig. 17. Load-deflection curves (41-5 to 45-5).

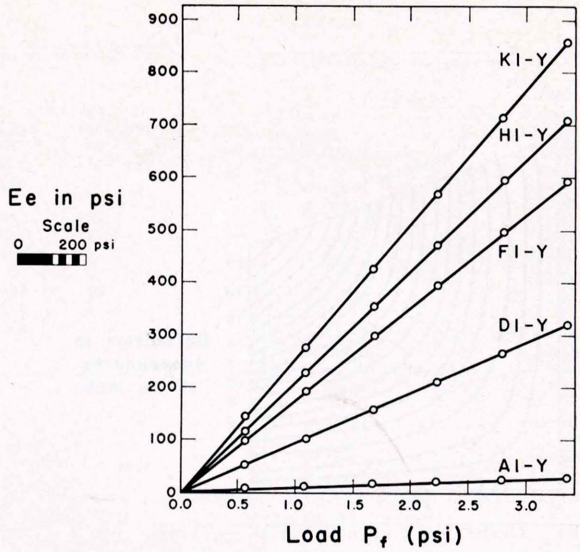

Fig. 18. Load Ee curves (A1—Y to K1—Y).

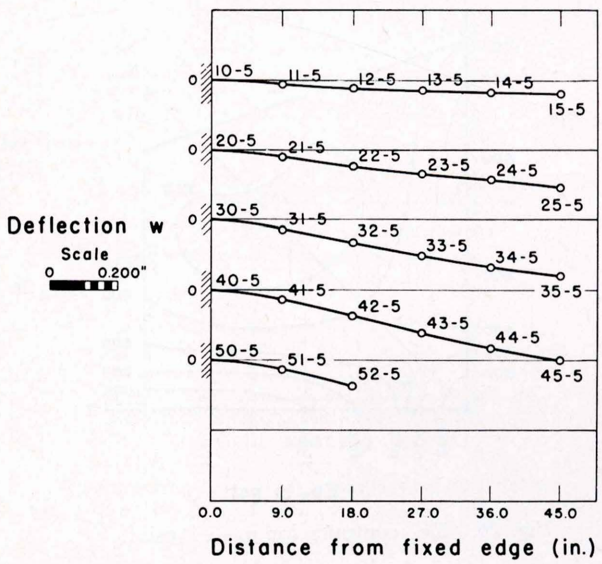

Fig. 19. Deflection sections parallel to x-axis.

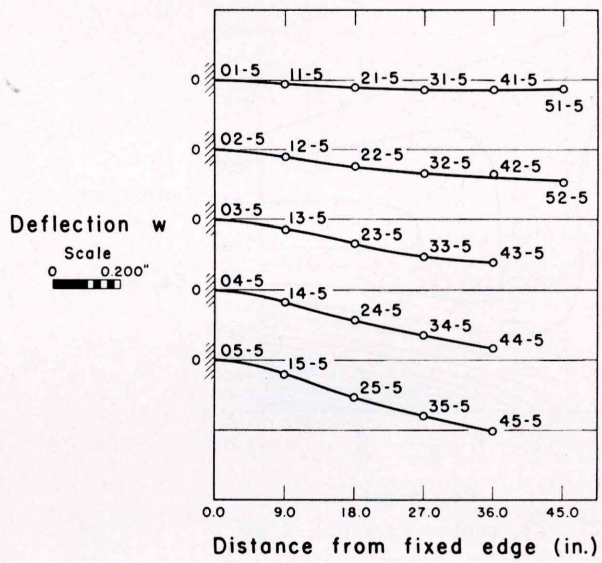

Fig. 20. Deflection sections parallel to y-axis.

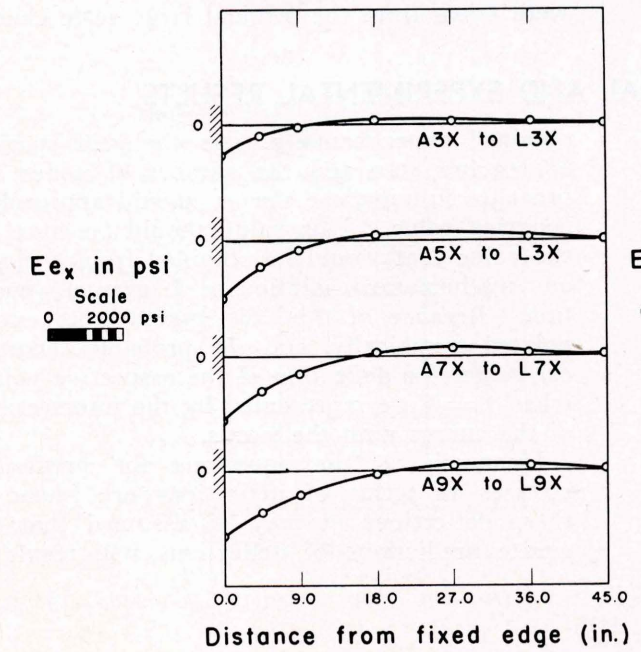

Fig. 21. Ee sections parallel to x-axis.

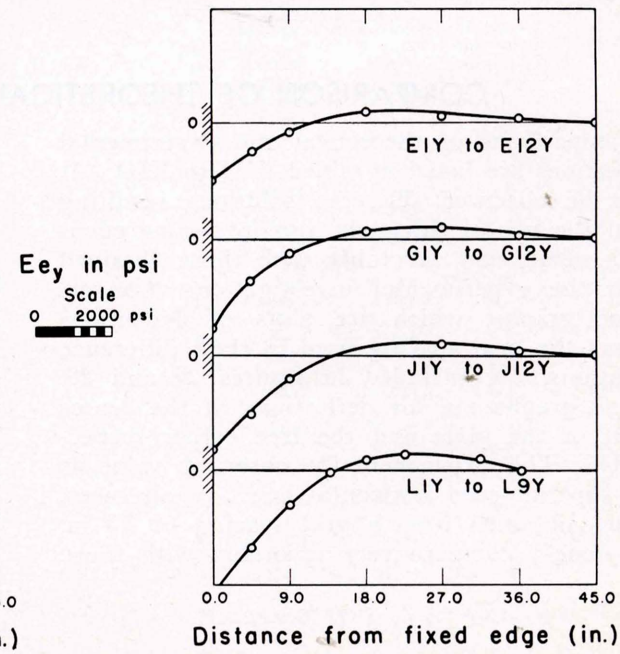

Fig. 22. Ee sections parallel to y-axis.

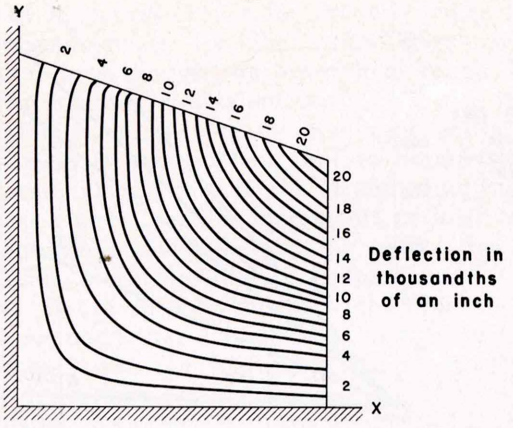

Fig. 23. Deflection contours for $p_f = 1$ psi.

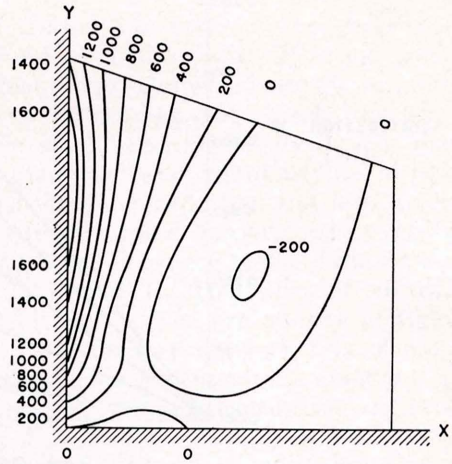

Fig. 24. Ee_x contours for $p_f = 1$ psi.

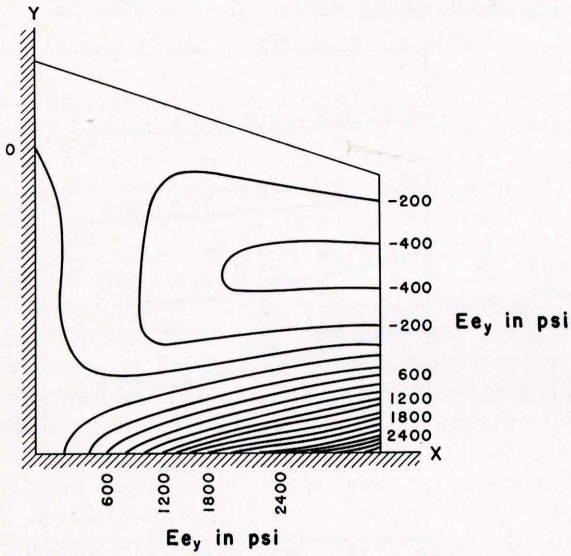

Fig. 25. Ee_y contours for $p_f = 1$ psi.

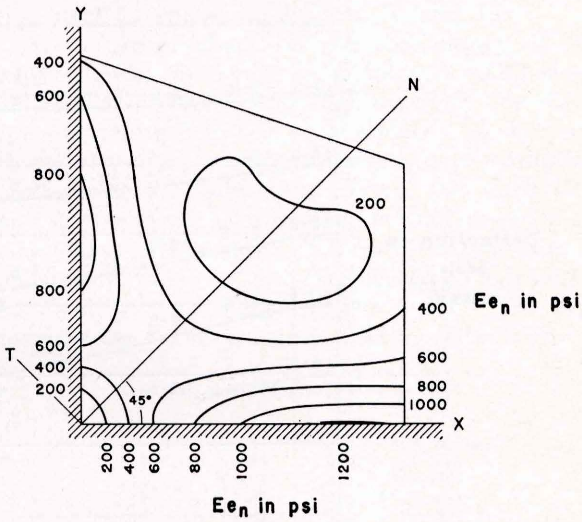

Fig. 26. Ee_n contours for $p_f = 1$ psi.

miniatures of which are shown in figures 23 to 26, give another check on the consistency of experimental observations. All values for comparison of results of experimental with theoretical were taken from the original large scale charts.

COMPARISON OF THEORETICAL AND EXPERIMENTAL RESULTS

Comparisons of theoretical and experimental deflections are listed in tables VIII to XIII. It may be observed that the solutions resulting from the use of thirty-six and forty-nine equations agree very favorably with those obtained from the experimental investigation. Convergence graphs, which are plots of deflections versus the grid spacing used in their difference equations, are included in figures 27 and 28. These graphs are for deflections at the center point of the plate and the free corner respectively. The experimentally observed value is the superimposed horizontal line. In all cases, values obtained from a grid spacing of 7.5 in. (36 nodes) compare very favorably with those obtained experimentally. As the grid spacing approaches zero and the number of nodes approaches infinity, the results should approach a constant value. This value should be equal to the value that would be obtained from a rigorous mathematical solution of Lagrange's equation. Because of this, the curves were extrapolated graphically, and the probable theoretical values for deflection of the respective points when $\lambda = 0$ are represented by the intersections of the curves with the y-axis.

Inasmuch as the equations for predicting stresses in terms of deflections are linear in these deflections, it may be assumed that accurate predictions of deflections will result in

Table VIII. Deflection comparisons for 2 x 2 grid.

	Deflection (in.)		
Node	Theoretical $p_f=1$ psi	Experimental $p_f=1$ psi	Percent[a] difference
11	0.11066	0.069	59.0
12	0.18789	0.134	34.0
21	0.13220	0.104	27.0
22	0.25287	0.228	11.0

[a]Based on experimental.

Table IX. Deflection comparisons for 3 x 3 grid.

	Deflection (in.)		
Node	Theoretical $p_f=1$ psi	Experimental $p_f=1$ psi	Percent[a] difference
11	0.04453	0.027	65.2
12	0.08259	0.060	37.3
13	0.11197	0.082	36.0
21	0.06869	0.052	32.0
22	0.14315	0.120	19.0
23	0.20415	0.175	17.0
31	0.07641	0.055	39.0
32	0.17480	0.154	13.0
33	0.25509	0.228	12.0

[a]Based on experimental.

Table X. Deflection comparisons for 4 x 4 grid.

	Deflection (in.)		
Node	Theoretical $p_f=1$ psi	Experimental $p_f=1$ psi	Percent[a] difference
11	0.02019	0.015	37.0
12	0.04059	0.030	32.5
13	0.05564	0.043	28.0
14	0.06397	0.055	25.0
21	0.03620	0.028	29.0
22	0.08072	0.069	17.0
23	0.11763	0.105	12.0
24	0.15065	0.134	12.0
31	0.04297	0.035	23.0
32	0.10391	0.093	12.0
33	0.15867	0.148	7.0
34	0.20692	0.193	7.0
41	0.04584	0.036	12.7
42	0.11914	0.104	11.4
43	0.18769	0.172	10.9
44	0.24530	0.228	7.5

[a]Based on experimental.

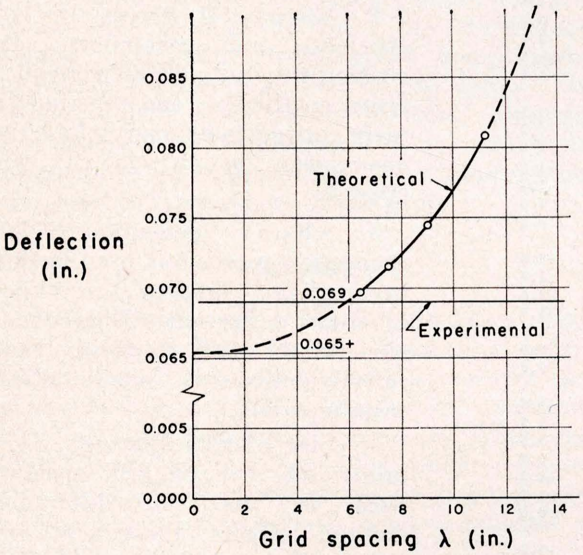

Fig. 27. Convergence graph for deflection at center of ½ in. plate for $p_f = 1$ psi.

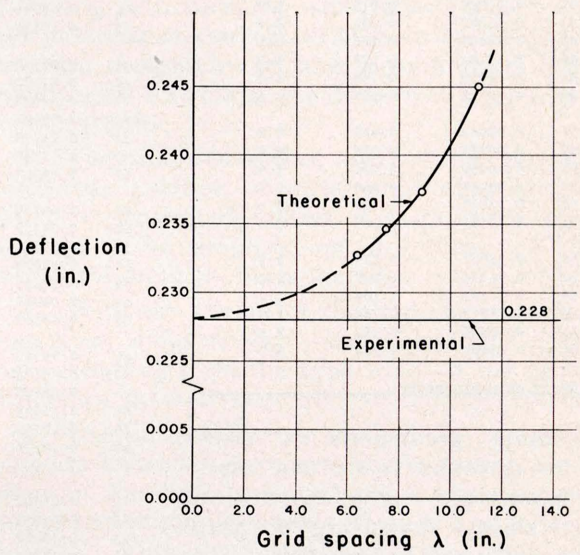

Fig. 28. Convergence graph for deflection at free corner for $p_f = 1$ psi.

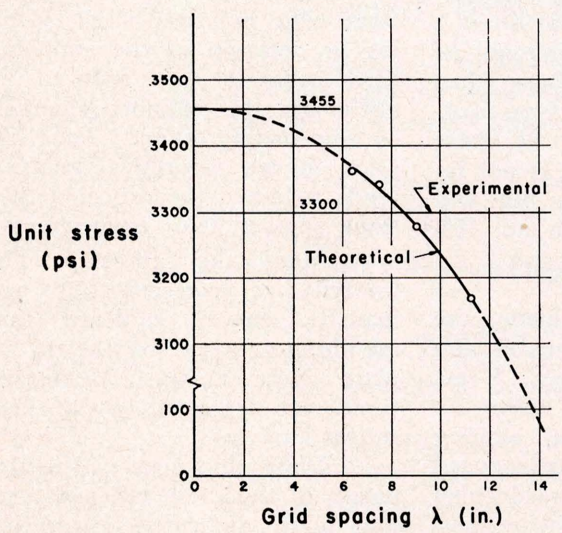

Fig. 29. Convergence graph for stress at L1—Y.

Table XI. Deflection comparisons for 5 x 5 grid.

	Deflection (in.)		
Node	Theoretical $p_f=1$ psi	Experimental $p_f=1$ psi	Percent[a] difference
11	0.01035	0.009	13.0
12	0.02220	0.019	17.0
13	0.03144	0.028	12.5
14	0.03881	0.035	11.0
15	0.04566	0.040	14.0
21	0.02055	0.018	14.0
22	0.04828	0.045	7.5
23	0.07258	0.069	5.0
24	0.09279	0.087	6.5
25	0.11214	0.105	7.0
31	0.02620	0.025	5.0
32	0.06609	0.062	6.8
33	0.10404	0.100	4.0
34	0.13687	0.132	3.0
35	0.16783	0.160	4.0
41	0.02862	9.028	2.0
42	0.07647	0.072	6.0
43	0.12490	0.120	4.0
44	0.16782	0.165	4.8
45	0.20712	0.202	2.5
51	0.02956	0.025	18.0
52	0.08417	0.073	15.0
53	0.14170	0.144	-2.2
54	0.19272	0.188	2.5
55	0.23716	0.228	4.0

[a]Based on experimental.

Table XII. Deflection comparisons for 6 x 6 grid.

Node	Deflection (in.) Theoretical p_f=1 psi	Deflection (in.) Experimental p_f=1 psi	Percent[a] difference
11	0.00583	0.006	-2.8
12	0.01321	0.012	6.0
13	0.01938	0.019	2.0
14	0.02422	0.023	6.0
15	0.02849	0.027	5.5
16	0.03233	0.031	4.5
21	0.01250	0.012	4.0
22	0.03069	0.027	12.0
23	0.04756	0.045	5.6
24	0.06172	0.060	2.8
25	0.07413	0.070	6.0
26	0.08636	0.082	5.0
31	0.01697	0.017	-0.5
32	0.04433	0.043	3.0
33	0.07167	0.069	4.0
34	0.09575	0.095	1.0
35	0.11714	0.114	3.0
36	0.13825	0.134	3.0
41	0.01927	0.019	1.0
42	0.05299	0.052	2.0
43	0.08869	0.088	0.5
44	0.12141	0.120	1.0
45	0.15079	0.149	1.0
46	0.17922	0.175	2.5
51	0.02042	0.019	7.5
52	0.05847	0.055	6.0
53	0.10066	0.098	2.5
54	0.14042	0.140	0.5
55	0.17619	0.177	-0.5
56	0.20981	0.207	2.0
61	0.02061	0.019	8.5
62	0.06274	0.055	14.0
63	0.11107	0.104	7.0
64	0.15715	0.154	2.0
65	0.19806	0.197	0.5
66	0.23484	0.228	3.0

[a]Based on experimental.

Table XIII. Deflection comparisons for 7 x 7 grid.

Node	Deflection (in.) Theoretical p_f=1 psi	Deflection (in.) Experimental p_f=1 psi	Percent[a] difference
11	0.00351	0.004	-13.0
12	0.00836	0.009	-7.0
13	0.01265	0.013	-3.0
14	0.01609	0.018	-10.8
15	0.01896	0.020	-5.8
16	0.02170	0.023	-5.5
17	0.02391	0.025	-4.4
21	0.00801	0.009	-8.8
22	0.02040	0.019	7.0
23	0.03247	0.031	5.0
24	0.04286	0.043	-0.5
25	0.05175	0.052	-0.5
26	0.05993	0.059	1.5
27	0.06794	0.067	1.5
31	0.01144	0.012	-4.5
32	0.03075	0.029	6.0
33	0.05083	0.051	-0.5
34	0.06900	0.069	0.0
35	0.08496	0.087	-2.5
36	0.09961	0.100	-0.5
37	0.11438	0.113	1.0
41	0.01350	0.014	-3.5
42	0.03798	0.038	0.0
43	0.06480	0.066	-2.0
44	0.09007	0.091	-1.0
45	0.11278	0.114	-1.2
46	0.13370	0.133	1.0
47	0.15460	0.153	0.5
51	0.01459	0.016	-9.0
52	0.04260	0.042	1.5
53	0.07463	0.075	-0.5
54	0.10579	0.107	-1.3
55	0.13435	0.136	-1.0
56	0.16063	0.161	0.0
57	0.18637	0.185	0.5
61	0.01520	0.016	-6.5
62	0.04578	0.043	6.5
63	0.08198	0.079	3.5
64	0.11809	0.118	0.0
65	0.15155	0.153	-1.0
66	0.18215	0.185	-1.5
67	0.21133	0.211	0.0
71	0.01502	0.016	-5.0
72	0.04813	0.044	9.0
73	0.08857	0.082	7.0
74	0.12948	0.126	2.0
75	0.16737	0.167	0.0
76	0.20140	0.202	-0.5
77	0.23266	0.228	2.0

[a]Based on experimental.

Table XIV. Results of convergence graphs.

Nodes	Deflection, free-corner (in.)	Deflection, center (in.)	Stress Lly (psi)
4	0.253	0.111	----
9	0.255	-----	----
16	0.245	0.081	3170
25	0.237	0.075	3280
36	0.235	0.072	3340
49	0.233	0.070	3360
Experimental	0.228	0.069	3300
Theoretical	0.228	0.066	3450

accurate predictions of stress. This is found to be true of deflections are carried to at least five places. A convergence graph for stress at Lly, which is similar to those drawn for deflections, is included in figure 29. This curve was also extrapolated graphically so that the probable theoretical value for stress at Lly when $\lambda = 0$ is represented by the intersection of the curve with the y-axis. The results of this convergence graph in addition to those for deflection are presented in table XIV.

This investigation has been restricted to observing and predicting the structural behavior of a ½ in. aluminum plate of size shown in figure 12, when subjected to a normal distributed load varying linearly from the sloping edge. If it is assumed that reinforced concrete is homogeneous and of constant moment of inertia [19, p. 422], these results through the principles of similitude [9], may be used to predict the structural behavior of a reinforced concrete wingwall of geometrically similar shape when subjected to a similar type loading. The application of these principles of similitude is not included in this bulletin but will be indicated in bulletin no. 183.

DISCUSSION

Many items may influence the results of the experimental and theoretical investigations. A few of the more important follow:

1. Simplification of sloping edge. Since loading approached zero at this edge, it was decided this simplification would be justified. Ignoring other possible compensating errors the close agreement between the analytical and experimental results would indicate that this simplification is valid.

2. Round off errors in coefficients and remainders. In writing the finite-difference equations, coefficients and remainders were carried to as many places as convenient on an electric calculator.

3. Shear deflection. The theoretical method as used in this investigation ignores the effect of shear deflection. This omission would tend to make theoretical deflections smaller than experimental.

4. Size of grid spacing. Certainly the size of grid spacing used in the finite-difference method affects theoretical results. The convergence graphs, figures 27 to 29, indicate this effect.

5. Fixation of edges. Absolute fixation could not feasibly be reached in the model. Plots of observed strains down each fixed edge indicated slight yielding or rotation of the supports. Such rotation was reduced by stiffening the support channels on the loading frame. True fixation in the theoretical analysis tends to make theoretical deflections smaller than experimental.

6. Membrane forces. The linearity of load-deflection and load-Ee curves indicate that membrane forces for the ½ in. plate were small. Membrane forces are neglected in the theoretical analysis.

7. Plate thickness. Measurements of thickness taken at various points indicated a variation

of only 0.005 in. in 0.500 in. The plate was, therefore, considered to be of constant thickness.

8. Homogeneity of plate. Tensile tests of samples taken at right angles to each other indicated similar physical properties as assumed.

9. Simulation of distributed load. A sufficient number of individual concentrated loads was used to approximate the distributed load of the theoretical analysis.

10. Compensating gages. Unstressed specimens to which the SR-4 compensating gages were applied, because of their size, were more sensitive to rapid changes in air temperature than the aluminum plate. Lack of consistent zero readings on the SR-4 gages before and after test tended to confirm this. The SR-4 gages should have their temperature compensating gages on the opposite side of the plate. This would double the strain impulse, eliminate measurement of membrane strains, and better compensate for temperature. This improvement was used in later stages of the project.

SUMMARY

Authorization was given by the Iowa Highway Research Board to the Iowa Engineering Experiment Station to conduct a research program on the structural behavior of reinforced concrete bridge abutment wingwalls of the types built by the commission. This bulletin reports on stages one and two of a four stage project. Stages one and two have been conducted as follows:

1. An exhaustive review of literature was performed to determine if such a study had previously been made. No record of research of this type was discovered.

2. A questionnaire was distributed to several hundred highway, railway, and consulting engineers throughout the United States and Canada.

3. The result of the literature review and questionnaire survey which together were stage one of the project was that a thorough study of the subject was needed.

4. The method of finite differences was used to solve the Lagrange plate equation written for a plate of the wingwall type.

5. Solutions were obtained corresponding to six different grid spacings.

6. The various solutions were compared with experimental results obtained by testing a ½ in. aluminum plate which was considered a model of a typical wingwall.

7. This comparison indicated that satisfactory predictions of structural behavior may be made from the set of equation corresponding to the 6 x 6 grid (36 simultaneous equations).

8. Stage three will use these findings to present moment contours for constant thickness bridge abutment wingwalls of the various proportions being used by the Iowa State Highway Commission. This stage will be reported in bulletin 183.

9. Stage four will provide an analytical procedure for the structural analysis of variable thickness wingwalls. A typical variable thickness wingwall will be analyzed for moments. This stage will be reported in bulletin 184.

CONCLUSIONS

1. A rigorous mathematical solution of the governing differential equations for many engineering structures by structural engineers is not practical or convenient because of the mathematical complexity of such a solution as compared with numerical methods which give adequate results.

2. The finite-difference method for the approximate solution of differential equations of the types commonly found in engineering phenomena is the simplest and most direct of the numerical methods investigated.

3. With the advent of the high speed digital computer, simultaneous linear algebraic equations resulting from the application of the finite-difference method may be economically solved.

4. The finite-difference method for prediction of plate behavior gives reasonable results for a plate of the type, restraints, and loading used in this investigation when a 36 node grid system is used. This conclusion was found to agree with that of previous investigators [4, p. 20].

> Using an analogous grid consisting of six north-south beams and six east-west beams and solving directly linear equations containing all three unknowns at each joint, . . . the computed center moment on a uniformly loaded square plate agrees remarkably well with Henri Marcus' solution by the theory of elasticity.

5. Many engineering problems may be solved through application of the finite-difference method coupled with high-speed digital comuters. A few of the more important of these types of problems have been outlined, [10].

6. The load system used very closely approximated that of a theoretically distributed load.

ACKNOWLEDGMENTS

During this investigation, many individuals have given advice and help, without which this study could not have been possible. The assistance of the following people is gratefully acknowleged.

The Iowa Highway Research Board, whose support made this project possible.

The following members of the Iowa State Hihway Commission: Bert Myers, Neil Welden, Welden, P. F. Barnard, and Mark Morris.

Dr. P. V. Faragher of the Aluminum Company of America furnished without charge the aluminum plates used in this investigation.

Dr. Max A. Woodbury, Principal Investigator on the Logistics Research Project, and George Stephenson, Director of the Computation Laboratory, George Washington University, Washington, D. C., were responsible for the gratis solutions of the sets of sixteen and forty-nine equations on the Navy's Logistics Computer.

REFERENCES CITED

1. Barton, M. V. Finite Difference Equations for the Analysis of Thin Rectangular Plates with Combinations of Fixed and Free Edges. CF—1005, DRL—175, Defense Research Laboratory, University of Texas, Austin, Texas. August 6, 1949. (Mimeo.)
2. Benjamin, J. R., Scordelis, A. C., and others. Discussion of Deflections in Gridworks and Slabs. American Society of Civil Engineers Proceedings. v. 78, D-89, Dec. 1952.
3. Bowen, G. and Shaffer, R. W. Flat Slab Solved by Model Analysis. American Concrete Institute Journal. 26: 553-570. 1955.
4. Ewell, W. W., Okubo, S. and Abrams, J. I. Deflections in Gridworks and Slabs. American Society of Civil Engineers Proceedings. v. 77, 89. Sept. 1951.
5. Jensen, V. P. Analysis of Skew Slabs. University of Illinois Experiment Station Bulletin No. 332, 1941.
6. Lee, G. H. An Introduction to Experimental Stress Analysis. Wiley, N. Y. 1950.
7. Marcus, I. H. Die Theorie elastischer Gewebe und ihre Anwedung auf die Berechnung biegsamer Platten. (The theory of the elastic web and its use for the calculation of flexible plates). Julius Springer, Berlin, 1924.
8. Murphy, G. Advanced Mechanics of Materials. McGraw-Hill, N. Y. 1946.
9. Murphy, G. Similitude in Engineering. Ronald, N. Y. 1950.
10. Parme, A. Solution of Difficult Structural Problems by Finite Differences. American Concrete Institute Journal. 22: 237-256. 1950.
11. Portland Cement Association. Concrete Bridge Details. The Association. Chicago. 1942.
12. Salvadori, G., Baron, M. L. Numerical Methods in Engineering. Prentice-Hall. N. Y. 1952.
13. Southwell, R. V. An Introduction to the Theory of Elasticity. Clarendon Press. Oxford. 1936.
14. Southwell, R. V. Relaxation Methods in Theoretical Physics. Clarendon Press. Oxford. 1946.
15. Timoshenko, S. Theory of Plates and Shells. McGraw-Hill. N. Y. 1940.
16. United States Bureau of Reclamation. Boulder Canyon Projects Final Report. Part V. Technical Investigations. Bulletin No. 1. Trial Load Method of Analyzing Arch Dams. Denver, Colorado. 1938.
17. Wang, Chi-Teh. Applied Elasticity. McGraw-Hill. N. Y. 1953.
18. Westergaard, H. M. Theory of Elasticity and Plasticity. Wiley. N. Y. 1952.
19. Wise, J. A. The Calculation of Flat Plates by the Elastic Web Method. American Concrete Institute Journal. 24: 408-422. 1928.

APPENDIX

IOWA STATE COLLEGE
OF AGRICULTURE AND MECHANIC ARTS
AMES, IOWA

IOWA ENGINEERING EXPERIMENT STATION

A research project on the structural behavior of wing walls of bridge abutments is being conducted by the Iowa Engineering Experiment Station under the sponsorship of the Iowa Highway Research Board. The purpose of this project is to study the structural behavior of typical reinforced concrete wing walls.

A search of the available literature on wing walls of bridge abutments has been conducted. Few of the references discovered gave any idea of the method of designing such walls. The suggestion most commonly made was to design the wall as a simple cantilever retaining wall and then either eliminate the connection to the breastwall by means of a construction joint, or simply ignore it and let the wall crack. We believe we can be of service to all engineers engaged in the design of such structures if we can assemble the information which may be available in organizations such as yours.

We are sending this letter and attached questionnaire to the various highway commissions, railroads, and consulting firms in the United States and Canada who might have occasion to design such structures. If you do not wish to answer this questionnaire personally, please have the person in your organization who is best qualified to do so.

Though you and your organization are very busy, we feel justified in asking you to take a little of your time to provide us with the information requested. We hope that the response to this request will provide us with material of such value that it can be published so that it will become available to the profession.

We shall appreciate any information you can supply us. If you would like to have it, we shall be glad to send you a copy of the report on this survey when it is completed.

Sincerely yours,

W. C. Alsmeyer

William C. Alsmeyer
Associate Professor of
Civil Engineering

Publications of the Iowa Engineering Experiment Station

The Iowa Engineering Experiment Station publishes reports of the results of completed projects in the form of technical bulletins. Other research results are published in the form of Engineering Reports.

Single copies of publications not out of print may be obtained free of charge, except as noted, upon request to the Director, Iowa Engineering Experiment Station, Ames, Iowa. The publications are available in many libraries. *Indicates out of print.

BULLETINS

No. 175. Rapid Control Tests for Bituminous Paving Mixtures. T. Y. Chu. 1953.

No. 176. Constants for Design of Continuous Girders with Abrupt Changes in Moments of Inertia. R. A. Caughey and R. S. Cebula. 1954.

No. 177. Elastic Stability of the Top Chord of a Three-Span Continuous Pony Truss Bridge. Frank Kerekes and C. L. Hulsbos. 1954.

No. 178. Universal Swing Curves for Two Machine Stability Problem with Multiple Switching. A. A. Fouad and W. B. Boast. 1956. ($1.00).

No. 179. The Survival of Swine Disease Organisms in the Heat Treatment of Garbage. E. R. Baumann, R. A. Packer, et al. 1957. ($1.45).

No. 180. Colorimetric Characteristics of Color Television Images Recorded on Black and White Film. W. L. Hughes. 1957. ($0.50)

No. 181. Parking Practices on College Campuses in the United States. L. H. Csanyi. 1958. ($0.50).

No. 182. Structural Behavior of a Plate Resembling a Constant Thickness Bridge Abutment Wingwall. H. P. Harrenstien and W. C. Alsmeyer 1959. ($0.75).

ENGINEERING REPORTS

No. 21. Mechanical Analysis of Soils. D. T. Davidson and associates. Reprints. 1954-1955.

No. 22. Further Papers of the Wisconsin Loess of Southwestern Iowa. D. T. Davidson and associates. Reprints. 1953-1954.

No. 23. Secondary Stresses in Buried High Pressure Lines. M. G. Spangler. Reprint. 1954-1955.

No. 24. The Use of Good English in Technical Writing. J. H. Bolton. Reprint. 1954-1955.

No. 25. Fertilizer Research, Part I. G. L. Bridger and associates. Reprints. 1955-1956.

No. 26. Bond Between Concrete and Steel. H. J. Gilkey, S. J. Chamberlin, and R. W. Beal. Reprints. 1956-1957. ($1.85).

No. 27. Fertilizer Research, Part II. G. L. Bridger, D. R. Boylan and associates. Reprints. 1957-1958. ($0.75).

No. 28. Plastics as Materials of Construction. L. K. Arnold. Reprint. 1957-1958. ($0.25).

No. 29. Flexural Strength of Hollow Unit Concrete Masonry Walls in the Horizontal Span. A. R. Livingston, et al. 1958-1959. ($0.50).

No. 30. Alcoholic Extraction of Vegetable Oils. R. K. Rao, L. K. Arnold and associates. Reprints. 1958-1959. ($0.75).

THE COLLEGE

The Iowa State College of Agriculture and Mechanic Arts conducts work in five major fields;

Agriculture

Engineering

Home Economics

Science

Veterinary Medicine

The Graduate College conducts research and instruction in all these fields.

Four-year and five-year collegiate curricula are offered in the different divisions of the College. Non-degree programs are offered in agriculture. Summer sessions include graduate and collegiate work. Short courses are offered throughout the year.

Extension courses are conducted at various points throughout the State.

The College has five special research institutions: the Agricultural and Engineering Experiment Stations, the Veterinary Medical and Industrial Science Research Institutes, and the Institute for Atomic Research.

Special announcements of the different branches of the work are supplied, free of charge, on application.

Address, THE REGISTRAR, THE IOWA STATE COLLEGE, Ames, Iowa.